Article

Geological and Geotechnical Studies Aimed at the Project and Construction of Rockfill Recharge Dams: The Case Study of the Wadi Sulayf Dam, Wilayat Ibri Region, Oman

Vincenzo Canzoneri [1], Alessandro Bonfardeci [2], Simona Bongiovanni [2], Lavinia Coletta [3], Enrico Paolo Curcuruto [2], Maurizio Gasparo Morticelli [2], Attilio Sulli [2] and Alessandro Canzoneri [2,*]

[1] SERING Ingegneria, 90139 Palermo, Italy; vincenzo.canzoneri@sering.it
[2] Dipartimento di Scienze della Terra e del Mare, Università di Palermo, 90123 Palermo, Italy; alessandro.bonfardeci@unipa.it (A.B.); simona.bongiovanni@unipa.it (S.B.); enricopaolo.curcuruto@unipa.it (E.P.C.); maurizio.gasparo@unipa.it (M.G.M.); attilio.sulli@unipa.it (A.S.)
[3] SYSTRA, 7500 Paris, Ile-de-France, France; laviniacoletta.lc@gmail.com
* Correspondence: alessandro.canzoneri@unipa.it

Abstract: In recent years the Government of the Sultanate of Oman has planned the construction of recharge dams in the semi-desert region of Wilayat Ibri, according to the growing domestic water demand for drinking and agricultural use. For this reason, the Engineering Company SERING International planned the construction of rockfill dams, well positioned according to the local morphological and geological context. Using temporary floodwaters and releasing them slowly downstream, these dams increase the water flow of the Aflaj. The latter is the existing traditional irrigation system devised to manage the scarce water resources of the Sultanate. In this paper, we describe the IBRI 14 Dam, namely Wadi Sulayf Dam, with a total length of about 3200 m and lying close to the settlements of Ibri Town, the largest one among those projected. This paper shows the criteria that guided the design studies of the dam linked to the geological and geotechnical features of the area, the main dam characteristic and the activities developed until the work was completed in 2020. This work represents an interesting and useful case study about the complete cycle of realization of a dam, in particular considering that it had been affected by huge flooding during the construction but reporting no significant damage.

Keywords: recharge rockfill dam; geological and geotechnical investigations; geotechnical design; floods/water management

1. Introduction

The Sultanate of Oman is an arid and semi-arid country located in the southeastern corner of the Arabian Peninsula and represents a typical example of an arid climate (Figure 1a). The landscape, predominantly desert, is characterized by "wadi", an Arabic term indicating beds of dry rivers or valleys in which water flows only after heavy rains. During this events, humid oasis environments with natural pools and lush vegetation are created in the middle of the desert.

The Sultanate experiences an average precipitation of less than 250 mm per year and no precipitation at all in some years [1,2]. However, water demand is rising steadily,

driven by industrial and agricultural expansion as well as the increasing living standards of the population [3].

In 2008, the Ministry of Regional Municipalities and Water Resources (MRMWR), with the population expected to rise to over three and a half million by 2020, projected a growth in domestic and municipal water demand of over 50% (80–100 Mm³/year) [4]. Moreover, according to a 2016 forecast, water demand is expected to further increase during the next 20 years from 2.85 to 330 Mm³/yr due to population growth [5].

The Sultanate has a deep-rooted history, with people strongly attached to their rich cultural heritage, and they value water in various aspects of their lives [6]. For this reason, Oman has always dealt with the challenges imposed by the water situation, undertaking an active policy of sustainable development and keeping a constant focus on water resource saving. To manage its scarce water resources, a traditional irrigation system called "Aflaj" (plural of Falaj) was previously devised [7]. The Aflaj system can be described as an integrated system that collects groundwater, natural spring water, or surface water and delivers it by means of underground or surface channels, using the force of gravity alone, for domestic and agricultural purpose [6]. The water is distributed through irrigation channels to individual agricultural holdings (Figure 1b). The origins of this irrigation system in Oman may date back to 500 AD. Still, archeological evidence suggests that irrigation systems existed in this semi-arid area as early as 2500 BC [8,9]. Since 2006, five Aflaj irrigation systems have been inscribed in the UNESCO World Heritage List [6,10].

Maps of Aflaj positions can be obtained by consulting the official website of the Ministry of Agriculture, Fisheries and Water resources (MAFWR) of Oman [11].

More than 27% of Oman Aflaj are classified as inactive or non-exploitable [4,12]. The distribution and the status of Aflaj referring to 2001 in Oman regions were illustrated in a previous study [12]. These systems dried due to several factors, not only hydrophysical, but also socio-economic, among which we can mention the large number of new farms affecting the aquifer that feeds the Aflaj. Aflaj flow was reduced, and it dried out in some cases.

The increase in water consumption in various sectors and the lack of balance between supply and demand may lead to critical situations, also related to the already-mentioned problems that affected the Aflaj system. Since the availability of surface water is very limited in various regions, groundwater is often the only reliable source of fresh water. Therefore, intensive withdrawal of natural groundwater occurs despite natural aquifer recharge due to sporadic rainfalls. This exploitation resulted in a progressive lowering of the water table within alluvial aquifers; thus, a sustainable water supply is endangered or even impossible.

Considering all these factors in Oman, as in several arid regions, the management of water resources is crucial for the well-being of local communities. In this context, the decreasing groundwater resources can be addressed by taking steps to increase the natural groundwater recharge. In this way, another fundamental goal is to collect a greater amount of water by capturing natural water resource supplies, such as heavy rain and floods. Following this aim, a National Water Resources Master Plan has been prepared by the Ministry of Regional Municipalities & Water Resources (MRMWR) to establish a strategy for the sustainable development, management, and conservation of water resources [4].

In this context, the Government of the Sultanate has wisely chosen to improve the aquifers' recharge by implementing a wide network of groundwater recharge dams. The principle behind these works is based on the recharge of aquifers through the construction of small, relatively inexpensive dams well-positioned according to the local morphological and geological settings. These dams temporarily stop the flood flow and slowly release it toward the recharge zone [13,14].
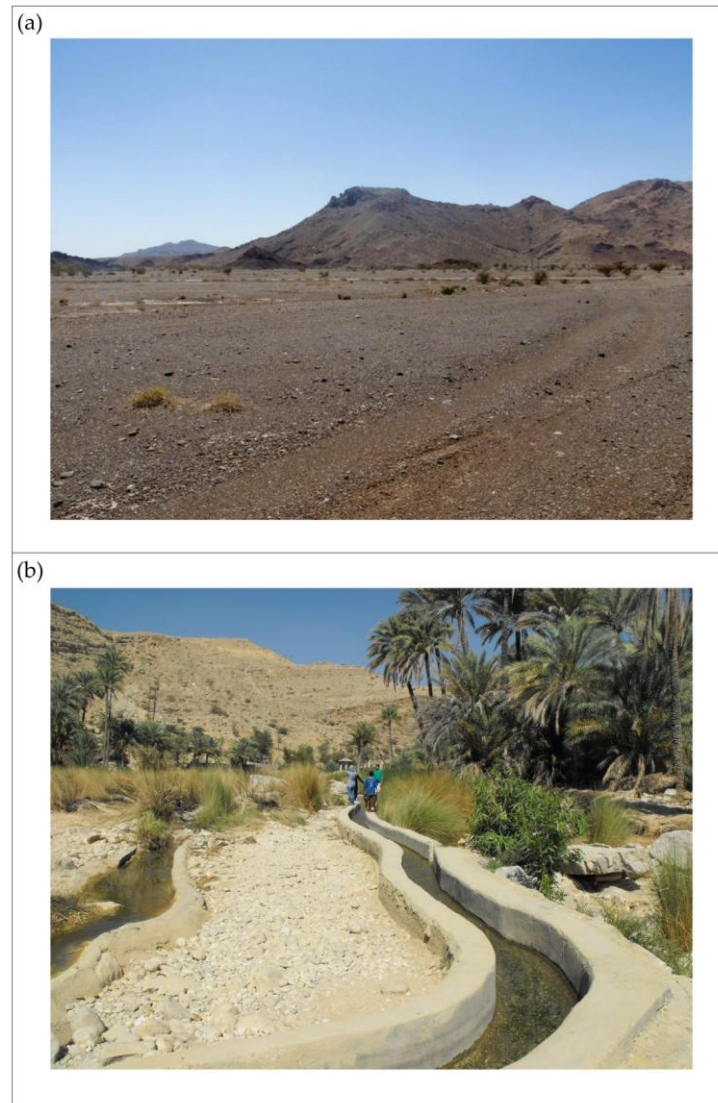
Figure 1. (**a**) Overview of the Wadi Sulayf floodplain and the surrounding low mountains in the southeastern area. The image illustrates the semi-arid conditions characteristic of the study area; (**b**) a typical example of Falaj in Wadi Bani Khalid (Oman).

From the perspective of the Aflaj recovery, the construction of dams to recharge the aquifers appears to be a good way to better manage the Aflaj systems [13]. As a matter of fact, a rise in well-water level and water production was noted in the northeast mountain plains and ridges of the Sultanate because of the construction of some recharge dams. In these areas, due to the steep mountain slopes and narrow coastal ranges, most of the run-off would be lost at the coastal side of the mountain without recharge dams [15].

By the end of 2004, twenty-four recharge dams had been completed in the Sultanate; in most cases (over 70%), the spillways were constructed with gabions or rock armour, while in the remaining cases concrete lining or concrete weirs were used [4]. By the end of 2021, the number of recharge dams constructed had risen to fifty-six [16]. Some of these projects have been reported in the literature [3,15–22].

The goal of this paper is to outline the criteria that led SERING International to adopt the geological and geotechnical design of an efficient rockfill recharge dam. We specifically describe the main features of the IBRI 14 Dam, namely the Wadi Sulayf Dam, the largest of those designed, which can provide the most efficient recharging of groundwater.

Finally, we also present the results of the geotechnical assessments conducted during the construction of the dam, supervised by SERING International, which started in October 2018 and was completed in April 2020. Furthermore, in the final stages of construction, the dam was affected by two major floods without suffering significant damage. The dam's reasonable response to these events demonstrates the effectiveness of the design choices made and the excellent supervision carried out during the construction phase.

2. Geomorphological and Geological Setting

2.1. Dam Site Location and Storage Reservoir

The Ibri Region is located on the southwestern slopes of the central Oman Mountains, facing the central desert, about 250 km west/southwest of Muscat.

The IBRI 14 Dam project site is located along a wadi near the village of Sulayf, 9 km southeast of the town of Ibri.

The geography of the area consists of the undulating topography with mountains and wadi planes. In particular, Wadi Sulayf lies between the NW-SE multiple ridge of the Hamrat and Duru Range and the deeply incised NW-SE ridge of Fajrah (Figure 2). The alluvial plain of the Wadi Sulayf is mainly composed of sandy gravels and Conglomerates, whose elements derive from the erosion of the Hamrat ad Duru Range. In Figure 2a (red continuous line), the IBRI 14 Dam catchment is shown.

The dam is located close to a narrowing in the large floodplain of Wadi Sulayf, downstream to the confluence between Wadi Lusayl and Wadi Manqas (Figure 2a). The floodplain of Wadi Sulayf appears to be bordered by some low mountain alignments.

About 5 km downstream from the selected dam site, Wadi Sulayf runs through a threshold that causes the narrowing of the wadi bed. The threshold, likely of structural origin, appears as a vertical cut in the sedimentary Eocene units of the Fajrah Ridge (Figure 2). In these circumstances, the substratum tends to rise up approaching the threshold, which causes the alluvial deposits to thin. The concentration of the groundwater flow caused by this geomorphological asset is testified by the presence of farms, houses, and the town of Ibri, over the threshold.
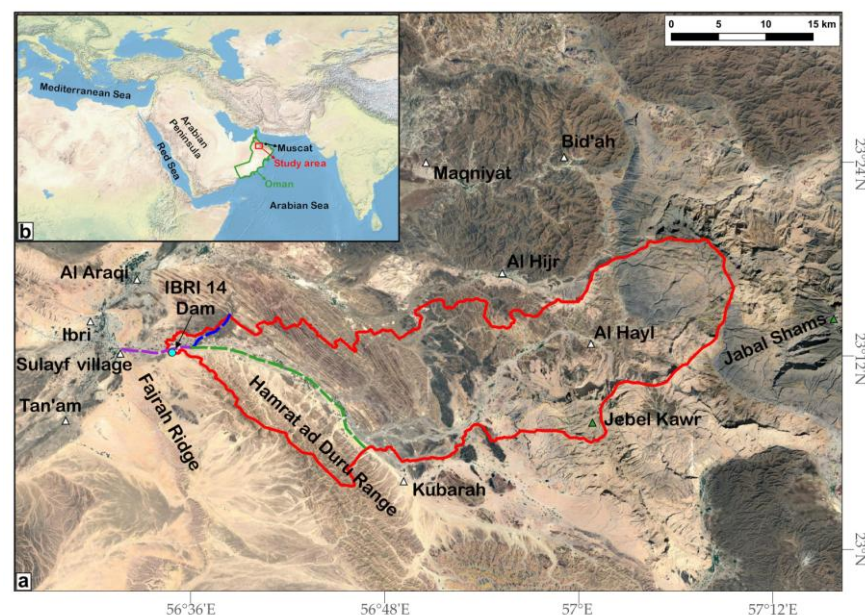

Figure 2. (**a**) View of the IBRI 14 Dam catchment area (red continuous line) and the river paths of the Wadi Lusayl (green dashed line), Wadi Manqas (blue dashed line), and Wadi Sulayf (purple dashed line); (**b**) location of the study area in the Arabian Peninsula and Oman territory. Map data

source: Google Earth, available online: https://earth.google.com/web/ (accessed on 4 October 2025) [23]; Coordinate reference system: WGS 84.

The main features of the catchment at the dam section are: a surface area of 770,260 km^2; stream length of 66.547 m; minimum altitude of 363 m a.s.l.; and maximum altitude 1012 m a.s.l.

2.2. Geological and Seismological Setting of Ibri Region

Oman is situated in the southeast corner of the Arabian Plate, with the Indian Plate to the east, the African Plate to the south/southwest, and the Eurasian Plate to the north/northeast. The stratigraphic and tectonic evolution of the Oman region is closely related to the progressive structuring of a Fold and Thrust Belt starting from the Late Cretaceous period, continuing to shorten and uplift until the Early Miocene [24,25]. As a result of the deformation of sequences from various paleogeographic domains, the Oman Mountains are the result of the piling-up of various tectonic units with main southwest vergency [26–32]. From bottom to top, the stratigraphy consists of autochthonous and para-autochthonous units of the crystalline basement with their sedimentary and volcanic covers (Late Proterozoic–Ordovician) and the Arabian carbonate platform succession (Middle Permian–Late Cretaceous). Tectonically overlying these latter layers are the Sumeini and Hawasina nappes, consisting of slope and basin deposits (Permian–Cretaceous), and the Semail ophiolitic complex (Cretaceous), which represents a fragment of Neo-Tethys oceanic crust obducted onto the Arabian continental margin. Unconformably overlaying these units, Neo-Autochthonous deposits made up of Late Cretaceous–Early Miocene hemipelagic and neritic sequences are present.

The geological sketch map shown in Figure 3 was redrawn starting from the NF 40-2F IBRI Geological Map Sheet (scale of 1:100,000), created by the Directorate General of Minerals, Ministry of Petroleum and Minerals [33]. The Ibri Region is characterized by the presence of allochthonous sedimentary rocks of the Hawasina Nappe, Late Permian–Cretaceous in age, Paleogenic Post-Nappe autochthonous rocks, and quaternary continental deposits [26,27,29,31,34].

In detail, three main geological units crop out in the region (Figure 3):

- Allochthonous units of the Hamrat Duru Group, belonging to the Hawasina Nappe. In particular, deposits belonging to three distinct formations are presents: (i) shallow-water packstone (Gw) of the Guwayza Fm., Middle–Upper Jurassic in age; (ii) open-marine deposits consisting of mudstone with chert nodules and turbiditic wackestone/packstone with cherts of the Sid'r Fm. (Si), late Tithonian to early–middle Cenomanian in age; (iii) open-shelf to distal open-marine deposits of the Wahrah Fm., represented by whachestone/packstone, mudstones and cherts, and cherts with silicified mudstones (Wa), Middle Jurassic to Turonian in age.
- Post-Nappe autochthonous units represented by inner to outer marine platform deposits, late Paleocene to early Eocene in age. They include yellow mudstones (e1aLM3), massive nodular mudstone/wackestone (e1bL), and bedded packstone/grainstone (e1bL1).
- Quaternary continental deposits, including (i) ancient (Qgx) and sub-recent (Qgy) alluvial fans and terraces; (ii) khabra deposits consisting of silts and clays (Qky-z); (iii) recent to sub-recent eolian sands (Qsy-z); (iv) recent alluvial deposits of wadis (Qtgz).
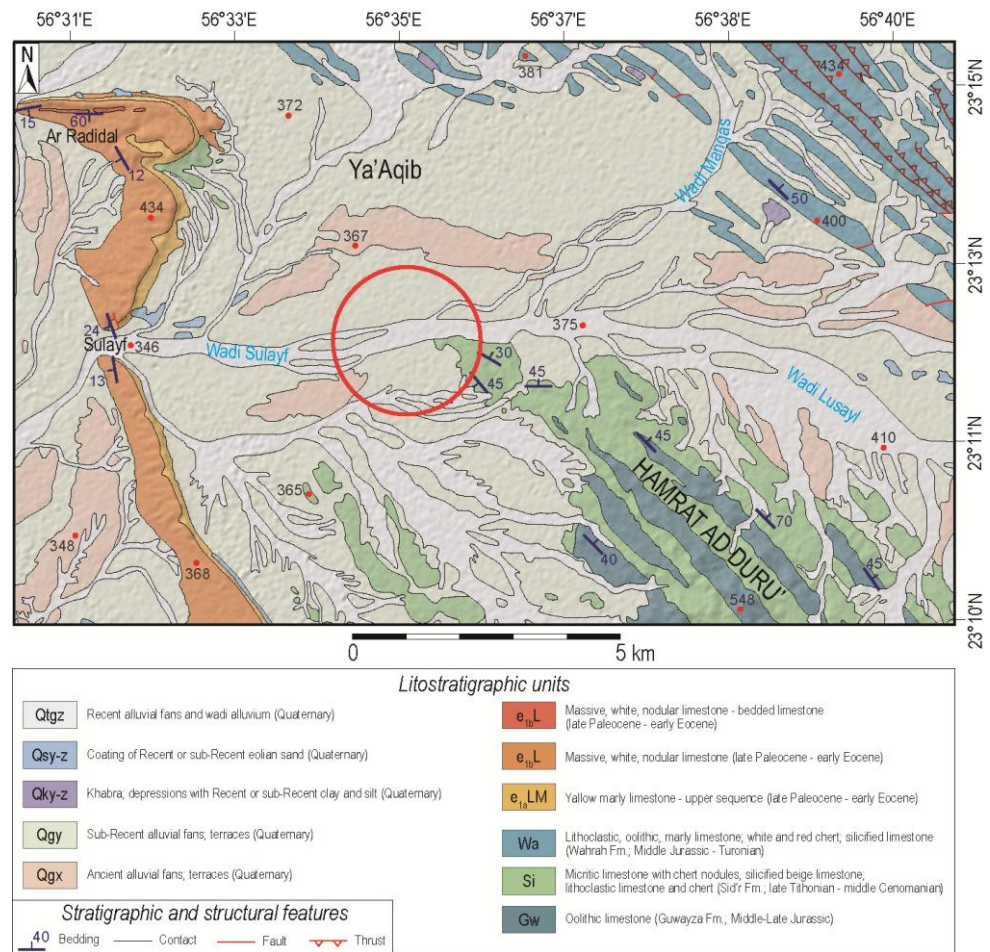
Figure 3. Geological sketch map of the study area redrawn from 1:100,000 Map Sheet NF 40-2F IBRI of Directorate General of Minerals, Ministry of Petroleum and Minerals [33]. The map was elaborated with GIS software (QGIS v. 3.30) [35], using a DEM image (30 m resolution) as topographic support (NAS Shuttle Radar Topography Mission (STRM) Global (2013) [36]. Distributed by OpenTopography. https://doi.org/10.5069/G9445JDF. Accessed on 2 October 2025). The red circle in the map indicates the location of the IBRI 14 Dam site.

3. Materials and Methods

According to various protocols and previous studies regarding rockfill recharge dam works, different materials and methodologies have been adopted during the feasibility study, detailed design, and supervision phase.

3.1. Feasibility Study and Detailed Design Phase

3.1.1. Recharge Dam Selection Criteria

Managed Aquifer Recharge (MAR) to improve the security and quality of water supplies in water-scarce areas holds enormous potential especially for village in semi-arid and arid areas [13]. However, for such projects to be successful, they must be well-planned, properly designed, and managed, and should be an integral part of water management strategies at the catchment/river basin level.

The checklist summarizing the aspects to consider when evaluating the applicability of MAR as part of a water management strategy is described in ref. [13] and in the databases [28,37].

Key aspects to consider include (i) identifying the potential water sources; (ii) assessing site suitability; (iii) selecting appropriate groundwater recharge methods; and (iv) assessing the associated benefits [13,38,39].

According to [13,38,39], the selection of the sustainable IBRI 14 Dam site was based on the following criteria:

- Local people request and presence of Aflaj.
- Catchment size: A large catchment basin is able to collect the volume of water in the recharge area. The fundamental principle of the identification is to identify dam sites that could perform the magnification of aquifer recharge in the indicated catchments and in the sub-catchment; the most promising situation is where the morphology shows a narrowing of the valley, with the consequent, presumable concentration of transit of groundwater avoiding the recharge dispersion in a too-large aquifer system [39]. This condition should optimize the piezometric elevation, creating better conditions for recovery of Aflaj systems or wells.
- The availability of alluvial deposit, holding the dam, which should possibly be constituted by permeable coarse sediments (gravel and sand) that allow the quick infiltration to the aquifer without interruption by low transmissivity layers as silty, clayey, or cemented ones.
- The retention basin location should be upstream of the villages. The reservoir and dam extension should not take away from areas planned for more relevant developments. Furthermore, the submergence of houses must be avoided and the temporary submergence of any roads and crops must be reduced to a minimum.
- Local dam functionality, guaranteeing adequate temporary retention capacity and sufficient drainage area extension.
- Economical aspects for a dam approximately 8–10 m high.

3.1.2. On-Site Surveys

SERING International carried out and supervised the geological, hydrogeological, and the on-site geotechnical surveys to assess the foundation soils and construction materials during the Feasibility Study phase. The on-site surveys and investigations started in June 2013 and were completed in November 2013. They included the following:

- Four vertical boreholes with continuous coring (location in Figure 4);
- Rock Quality Designation (RQD) determined according to Deere and Deere [40];
- Eight Standard Penetration Tests (SPTs), carried out during drillings in accordance with BS 1377-9 [41];
- Four permeability tests along the boreholes, consisting of three packer permeability tests and two falling head permeability tests, in accordance with BS 5930 [42];
- Installation of one standpipe piezometer along borehole BH-01;
- Collection of 6 bulk and disturbed samples from the core drilling boxes;
- Twelve trial pits within the reservoir area of the proposed dam, with depths ranging from 0.60 m to 2.50 m b.g.l. (location in Figure 4);
- Two infiltration/percolation tests performed inside the trial pits in accordance with BS 6297 [43].

3.1.3. Laboratory Tests

Laboratory tests were carried out on soil and rock samples collected during on-site surveys. In detail, the investigations included the following:

- Grain size analyses performed following ASTM standard [44];
- Modified Proctor Compaction Tests in accordance with ASTM standard [45];
- Uniaxial Compressive Tests carried out according to ISRM standard [46];
- Point Load Tests performed following ISRM standard [47].

Moreover, particle size distribution [44] and Proctor tests [45] were carried out on material samples collected in the trial pits and used for the construction of the dam.
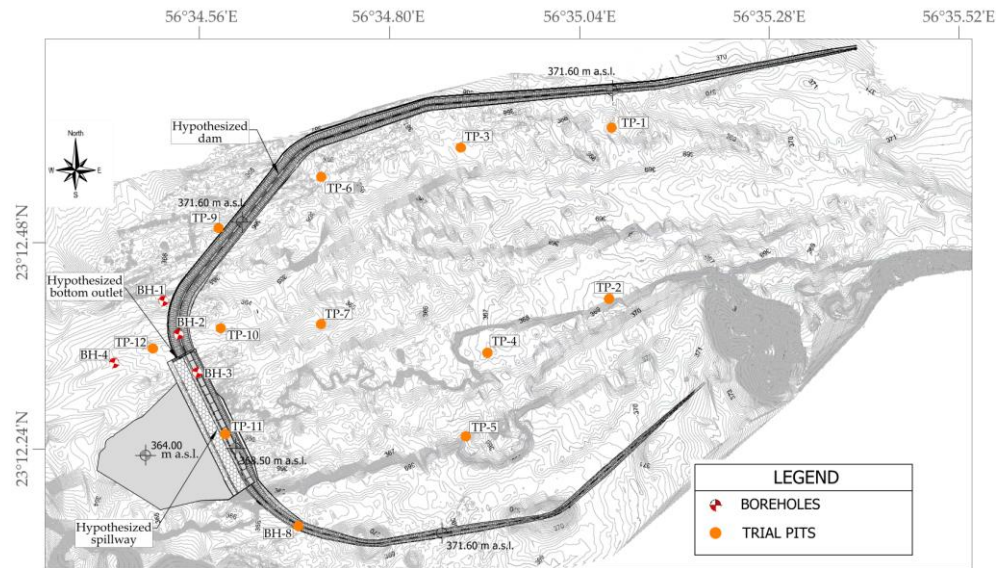
Figure 4. Location of the boreholes and trial pits. Elevation data are based on a detailed topographic survey carried out using GPS position system and total station (TS), provided by SERING International (Muscat, Oman). The isohypse equidistance is 0.1 m.

3.1.4. Geotechnical and Hydraulic Design

The detailed design of the dam was developed between 2014 and 2015 in accordance with the Omani Standards [48,49] and the main international regulations., e.g., [50–56].

The freeboard and the dam crest width were estimated following the criteria proposed in a previous study regarding the design of small dams [51].

To verify the stability of the interface between (i) drainage blanket and the granular fill of the shoulders, (ii) gabions and granular fill, (iii) transition and granular fill of the shoulders, and (iv) riprap and transition, the criteria proposed by Terzaghi [57] implemented by Sherard et al. [58,59] and USBR [51] were adopted. This approach is necessary to define the embankment zoning and to prevent internal erosion in the dam, as well as to define the correct dimension and location of filters, drains, and transition layers.

The riprap protecting the upstream dam slope was dimensioned according to Technical Release No. 69 [60], while the gradation limits were defined following the criteria of the U.S. Army Corps of Engineers [61].

The soil behaviour model adopted in the seepage analysis for the embankment zones, riprap, transition, and drainage blanket is the "Saturated/Unsaturated model" [62]. For this analysis, the embankment was modelled in SEEP/W (GEO-SLOPE International Ltd., Calgary, Canada, v. 2015 commercial product, https://www.adalta.it/geostudio/#SEEPW) [63].

Permeability functions were predicted using the Volumetric Water Content (VWC) functions of typical soil materials, in particular the grain-size estimation method of Kovács [64] modified by Aubertin et al. [65].

According to the literature, the recommended values of the safety factor for the exit gradient vary between 4 and 5 [50,52,66] or 2.5 and 3 [52,67].

The three foundation layers were assumed to be in a saturated stage, so they were assumed to have only saturated permeability.

A safety factor was applied to the critical hydraulic gradient (i_c) [50]:

$$i_c = \frac{\gamma'}{\gamma_w} \tag{1}$$

where γ' is the buoyant soil unit weight and γ_w is the water unit weight.

The safety factor against the quick condition for upheaval (*F_heave*), to account for foundation variations, is given by [50]:

$$F_{heave} = \frac{i_c}{i_e} \tag{2}$$

where i_e is the escape or exit gradient (predicted or measured) and consists of the maximum hydraulic gradient along the discharge boundary, the latter given analytically using the SEEP/W software (GEO-SLOPE International Ltd., Calgary, Canada, v. 2015, commercial product, https://www.adalta.it/geostudio/#SEEPW) [63].

Considering the difficulties associated with Modelling natural foundation soils and accurately assigning permeability values and other engineering properties, a safety factor of 4.0 was assumed [50,52,66,67] since this is the design of a new dam.

The overall stability of the upstream and downstream dam shoulders was assessed with the software SLOPE/W (GEO-SLOPE International Ltd., Calgary Canada, v. 2015, commercial product, https://www.adalta.it/geostudio/#SLOPEW) [68], using the Morgenstern–Price Method [69].

For the seismic characterization of the area, from the Global Seismic Hazard Map (GSHAM) [70], it was possible to estimate peak ground acceleration values between 1.6 and 2.4 m/sec². These values correspond to a 10% chance of exceedance for an exposure time of 50 years and a return period of 475 years, which is the standard approach for seismic hazard zonation studies.

The stability checks in the presence of seismic actions were carried out by means of the simplified pseudo-static method [71]. The design seismic inertia forces F_H and F_V acting on ground mass, for the horizontal and vertical directions, respectively, are taken as [72],

$$F_V = 0.5\alpha \times S \times W \tag{3}$$

$$F_V = \pm 0.5\, F_H \quad \text{if the ratio } \alpha_{vg}/\alpha_g \text{ is greater than 6} \tag{4}$$

$$F_V = \pm 0.33\, F_H \quad \text{if the ratio } \alpha_{vg}/\alpha_g \text{ is not greater than 6} \tag{5}$$

where α is the ratio of the design ground acceleration on type A ground (α_g), to the acceleration of gravity (g); α_{vg} is the design ground acceleration in the vertical direction; α_g is the design ground acceleration for type A ground; S is the soil parameter; and W is the weight of the sliding mass.

The maximum credible earthquake (MCE) and the operating basis earthquake (OBE) are defined in EM 1110-2-1806 [73]. The partial factor (γ_M) applied to the values of geotechnical parameters was established according to Eurocode 7 [55]. The minimum required safety factors (F_s) were derived from EM 1110-2-1902 [56] and EM 1110-2-1806 [73] protocols.

The Height/Surface Curve of the reservoir was determined according to the literature criteria [51,54]. The spillway was designed for a maximum flow rate according to EM 1110-2-1603 [74], while the bottom outlet was defined following indications from o EM 1110-2-1602 [75].

3.2. Supervision Phase

During the construction of the dam, both on-site and laboratory tests were conducted to analyze the appropriate use of materials and to validate the choices made during the design phase. In particular, field density determination according to ASTM standard [76] and permeability tests in the trial pits in accordance with BS standard [42] were performed on-site. The laboratory tests instead consisted of grain size analysis according to the ASTM standard [44] and Modified Proctor compaction tests in accordance with ASTM standards

[45]. Furthermore, filtration calculations were repeated following the procedures reported in Section 3.1.4.

4. Results

4.1. Geological Setting of the Dam Site

Based on the results of the geological survey and drillings, the detailed geological/geomorphological map of the IBRI 14 dam site (Figure 5) and two geological cross sections (longitudinal/orthogonal) along the dam (Figure 6b,c) were reconstructed.

The IBRI 14 Dam site area is characterized by Marls and limestones belonging to the Sid'r Formation (Hamrat Duru Group—Hawasina Nappes) overlain by recent, sub-recent, and ancient alluvial deposits and terraces (Figure 5).

The dam embankment and shoulders are settled on recent and cemented sub-recent alluvial deposits, whereas on the hydrographical left, downstream of the dam site, a terrace characterized by cemented ancient alluvial deposits is present.

The recent and the sub-recent alluvial deposits cover the wide plain bordered by low mountains. Upstream of the dam site, on the hydrographical left, the low mountains (ranging from 360 m to 560 m a.s.l.) are constituted by mudstone and turbiditic wackstone/packstone with cherts, belonging to the Sid'r Formation.

In particular, alluvial deposits consist of sub-rounded to sub-angular, medium-to-coarse grained gravels with some cobbles and boulders in a silty/sandy matrix. The elements that make up these alluvial deposits derive from the erosion and transport of a great variety of lithotypes cropping out in the large catchment area of the Manqas, Lusayl, and Sulayf Wadis (see Figures 2 and 3).

The lithotypes analyzed are in fact represented by carbonatic, bioclastic, and silicoclastic rocks belonging to the Wahrah and Sid'r Formations (Hamrat Duru Group—Hawasina Nappes), and tectonites, intrusive, and effusive rocks belonging to the Samail Ophiolitic Nappe.
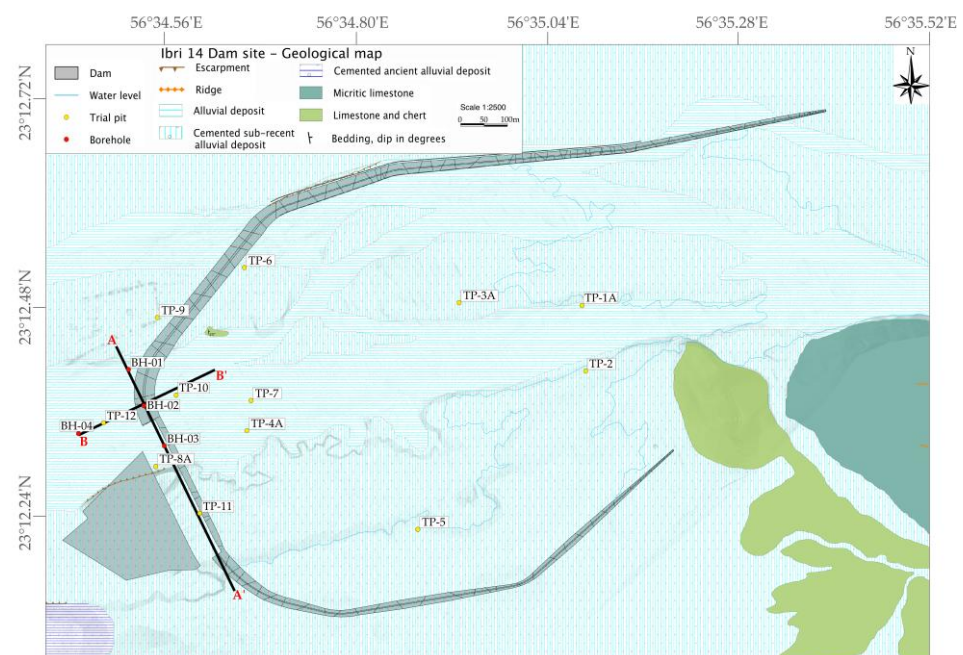

Figure 5. Geological/geomorphological map of IBRI 14 Dam site. The two black lines indicate the trace of the geological cross sections shown in Figure 6b,c. Elevation data are based on a detailed topographic survey carried out using GPS position system and total station (TS), provided by SERING International (Muscat, Oman).
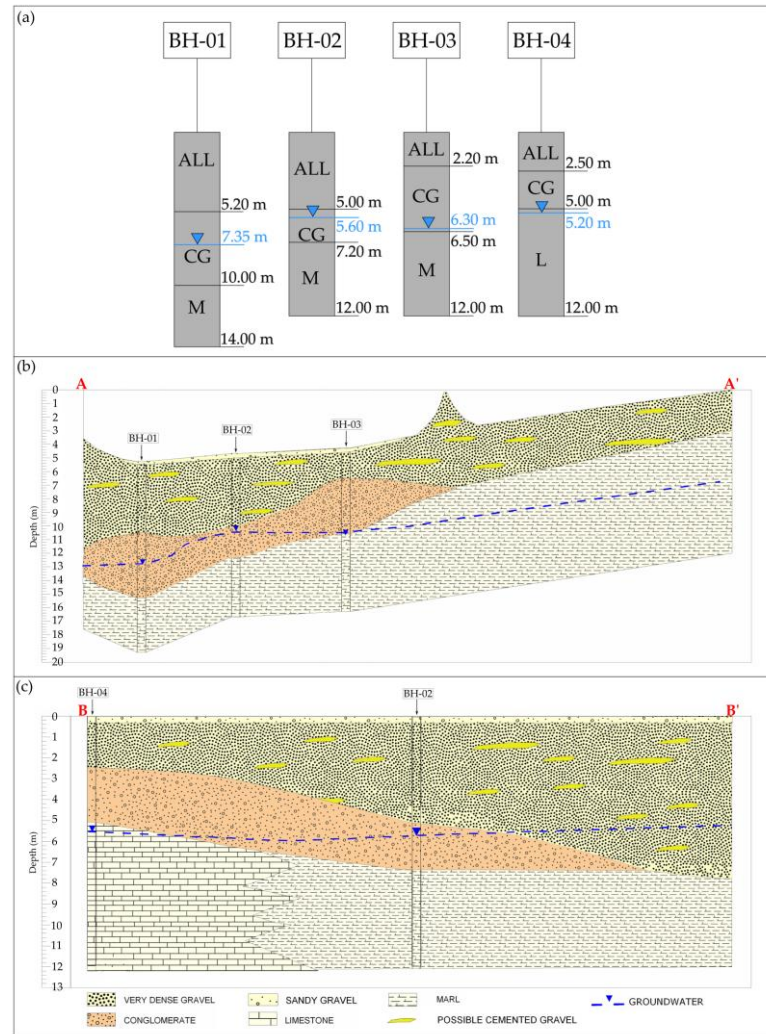
Figure 6. (**a**) Stratigraphic logs of the boreholes (location in Figures 4 and 5). The blue triangles indicate the water table level detected within the boreholes; (**b**) geological cross section AA' along the spillway of the IBRI 14 Dam (trace in Figure 5); (**c**) geological cross section BB' orthogonal to the embankment of the IBRI 14 Dam (trace in Figure 5).

4.2. Geotechnical Characterization of Foundations and Construction Materials

Field surveys, boreholes, trial pits, and laboratory tests allowed us to define the geotechnical characteristics of the foundation soils and construction materials of the selected dam site.

Four vertical boreholes with continuous coring were drilled, three of which (BH-02, BH-03, BH-04) (location in Figures 4 and 5) reached a depth of 12 m and one (BH-01) (location in Figures 4 and 5) 14 m below ground level. The water table level within the boreholes was detected between 5.20 and 7.35 m b.g.l.

The identified soils and rocks were grouped into four main units, as shown in the stratigraphic logs of the boreholes (Figure 6a):

- Alluvial Deposit (ALL);
- Conglomerate (CG);
- Marl (M);
- Limestone (L).

The identified units, their thickness within the boreholes, and the observed water table depths were also used to construct two geological cross sections: one longitudinal (Figure 6b) and one orthogonal (Figure 6c) to the IBRI 14 Dam.

As shown in the two geological cross sections (Figure 6b,c), the alluvial deposits consisting of sandy gravels, very dense gravels, and Conglomerates have an overall thickness varying between 5 and 10 metres, decreasing in the downstream sector and towards the hydrographical left of the watercourse. The Conglomerates are organized in lenticular bodies which are very variable in shape and size and are positioned in the lower part of the alluvial deposits. Their thickness varies between 2.20 and 4.80 m. The bedrock instead is represented by Marls and limestones unconformably overlain by the alluvial deposits with an estimated thickness of more than 10 m.

The water table resulted to be mainly contained in the Conglomeratic lenses and in the underlying weathered and fractured limestones and Marls.

4.2.1. Alluvial Deposit (ALL)

The wadi channel is filled with a very dense alluvial deposit (ALL) observed along all the boreholes and trial pits starting from ground level. A maximum thickness of 5.2 m was observed along boreholes BH-01 (location in Figures 4 and 5). The unit ALL consists of light-grey/light-off-white silty sandy gravel with rare cobbles and boulders. Gravel elements are medium-to-coarse grained with sub-rounded to sub-angular shapes. As shown in Figure 7, alluvial deposit (ALL) can be classified as sandy silt and gravel to silty sandy gravel [44].
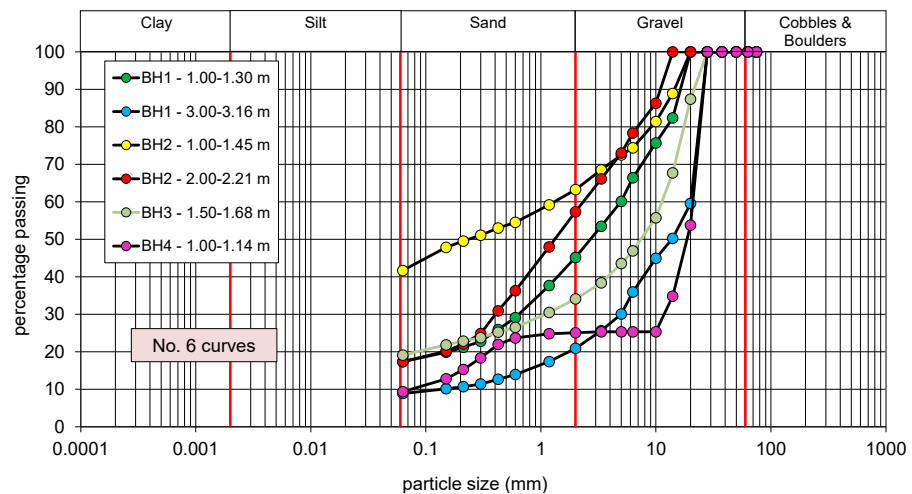

Figure 7. Grain size distribution curves of the alluvial deposit (ALL) ranging from sandy silt and gravel to silty sandy gravel. The red lines represent the boundaries between the grain size classes.

Geotechnical parameters derived from SPTs [41], including N_{SPT}, friction angle (φ), relative density (Dr), elasticity modulus (Es), shear wave velocity (Vs), and shear modulus (G_0) are shown in Table 1.

Table 1. Results of SPTs carried out in the alluvial deposit (ALL).

Borehole	Depth [m]	N_{SPT}	D_R (%)	φ (°)	E's	Vs [m/s]	G [m/s]
BH-01	1.00	50	100	46	73	262	112
BH-01	4.14	50	100	46	58	329	176
BH-02	1.00	37	100	46	48	235	90
BH-02	2.00	50	100	46	58	284	132
BH-03	1.50	50	100	46	58	268	118
BH-04	1.00	50	100	46	58	248	100
BH-04	3.00	32	92	45	44	286	133

The permeability of the alluvial deposit (ALL) was evaluated using the empirical approach of Hazen [77]. The apparent permeability values under unsaturated conditions range between 5.0×10^{-06} m/s and 1×10^{-05} m/s. This relevant alluvial deposit (ALL) represents the potential aquifer that could be alimented by the recharge dam.

The infiltration rate from in situ infiltration/percolation tests [43] conducted at depth of 0.60 m ranges between 0.72 mm/s and 1.73 mm/s.

4.2.2. Conglomerate (CG)

A moderately weak-to-strong, light-grey Conglomerate (CG) was observed continuously beneath the alluvial deposit (ALL), reaching a maximum thickness of about 5 m along boreholes BH-01 (location in Figures 4 and 5). CG unit was slightly to highly weathered and fractured, sometimes highly cemented. Fractures were sub-horizontal to horizontal, very closely to closely spaced, and occasionally medium spaced. RQD values [40] between 0% and 70% were measured corresponding to very poor to fair rock quality. The coefficient of permeability (k) ranged between 10^{-6} m/s and 10^{-7} m/s. Values of the Unconfined Compression Strength (UCS) between 9 MPa and 48 MPa were determined with Uniaxial Compressive Tests [46] and Point Load Tests [47].

During site investigations, the water table was systematically found within the Conglomerates (boreholes BH-01, BH-02) or at the base of the unit (BH-03, BH-04).

4.2.3. Marl (M)

Along the boreholes BH-01, BH-02, and BH-03 (locations in Figures 4 and 5), the bedrock consists of Marl (M) found from a depth of 6.3 to 10 m b.g.l. The Marl (M) is composed of stiff to hard, light-grey to reddish-brown, highly weathered silty clay, generally recovered in the dimension of gravel. Sometimes yellowish patinas were observed. RQD values [40] of 0% were measured generally, corresponding to very poor rock quality. The coefficient of permeability (k) obtained from Packer Tests [42] was about 10^{-6} m/s.

4.2.4. Limestone (L)

Along the borehole BH-04 (location in Figures 4 and 5) the bedrock consists of Limestone L. The unit are strong, light-off-white, fine grained, interbedded within the matrix of yellowish stained, and soft-to-firm sandy silt/silty sand. Very closely to closely spaced, occasionally medium spaced, sub-horizontal to horizontal fractures were observed. Fracture planes were smooth and regular, slightly to moderately weathered. RQD values [40] range from 0% and 44%, corresponding to very poor to poor rock quality. UCS values between 12 MPa and 24 MPa were determined with Uniaxial Compressive Tests [46] and Point Load Tests [47]. The coefficient of permeability (k) obtained from Falling Head Permeability Tests [42] was about 10^{-5} m/s.

4.2.5. Construction Materials

The presence of alluvial deposits (ALL), hereinafter referred to as gravel and sand (GS), to be used as granular fill in the dam embankment was confirmed within the dam basin by trial pits whose position is shown in Figure 4. In particular, light-grey, medium to coarse, sub-rounded to sub-angular silty sandy gravel with occasional cobbles was highlighted (Figure 8). Areas with cemented materials were frequently recognized. Levels of light-grey, fine to medium, silty, slightly gravelly sand were sometimes observed.

Figure 8. Gravel and sand (GS) observed along the Trial Pit 2 (TP-2) (location in Figures 4 and 5).

Due to the grain-size analyses [44], the samples were classified as silty sandy gravel (Figure 9a). The results of the Modified Proctor Compaction Tests [45] indicate a maximum dry density (γ_{dmax}) ranging between 2.20 and 2.25 t/m^3, with an optimum water content (w_{opt}) of about 6% (Figure 9b).
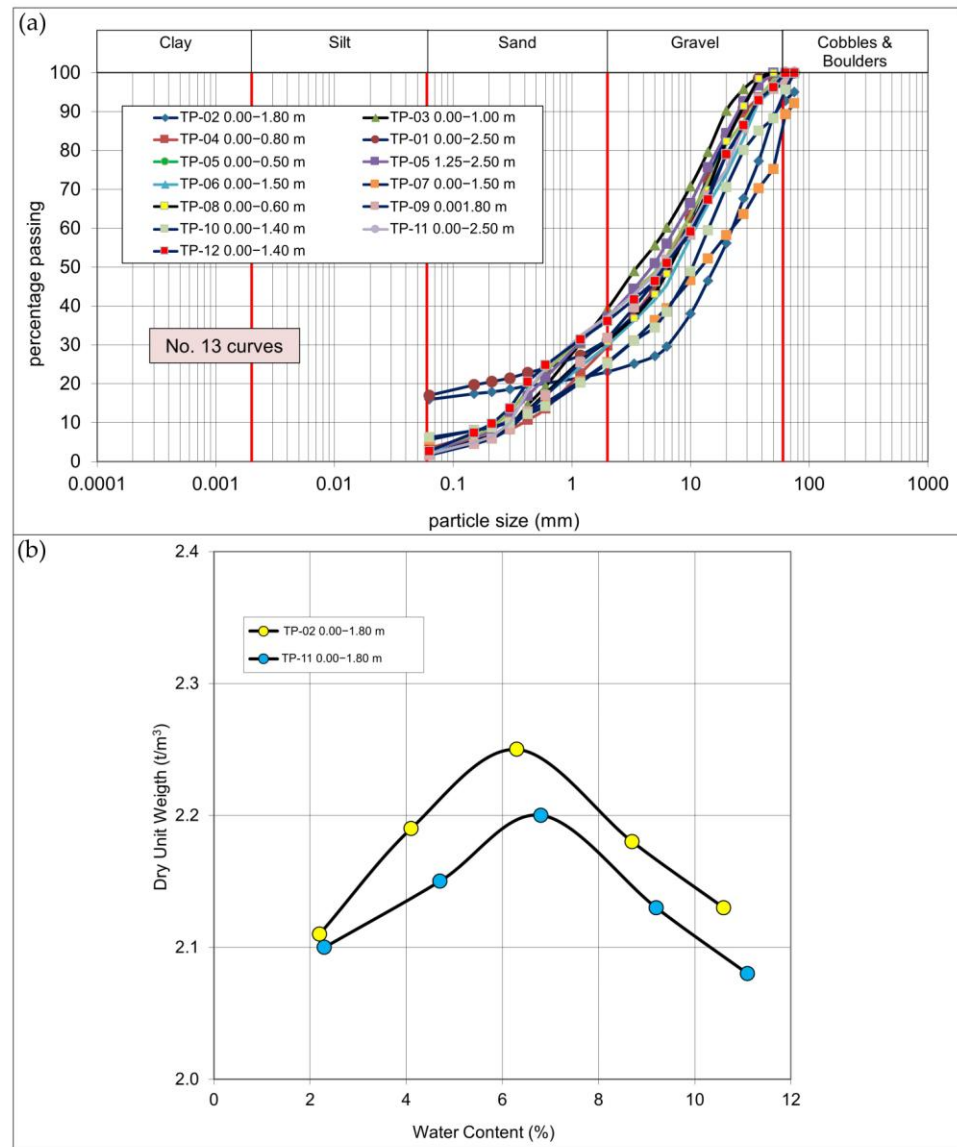
Figure 9. (**a**) Grain-size distribution curves of GS samples; (**b**) results of the Modified Proctor Compaction Tests on GS samples. The red lines represent the boundaries between the grain size classes.

4.2.6. Geotechnical Design Parameters

The geotechnical parameters (Table 2) assumed in the calculations were derived from the on-site results and laboratory tests.

Table 2. Mechanical parameters of foundation soils and rocks and construction materials.

Soil	Unit Weight γ (kN/m³)	Cohesion c′ (kPa)	Friction Angle φ′ (°)
Alluvial Deposits	21	0	35
Conglomerate	21	50	30
Marl/Limestone	20	15	28
Granular Fill	21	0	40
Riprap	23	0	45
Drainage Blanket	21	0	42

4.3. Geotechnical Design of the Dam Embankment

The detailed project was drawn up during the years 2014 and 2015. The following aspects are addressed.

4.3.1. Internal Erosion and Dam Slope Protection

The analyses to prevent internal erosion were carried out at the interface between (i) the drainage blanket and the granular fill of the shoulders; (ii) the gabions and the granular fill; (iii) the transition and the granular fill of the shoulders; and (iv) the riprap and the transition applying the appropriate criteria [51,57–59]. All verifications were satisfied, except for the stability at the interface between the gabions and the granular fill of the shoulders, where the inclusion of a geotextile layer was required to ensure adequate separation and stability.

Figure 10 shows the grain size distribution of the dam embankment materials, determined by applying the rules mentioned above. The granular fill consists of silty sandy gravel, and the drainage blanket is uniformly graded gravel. The riprap for dam slope protection consists of cobbles and the transition layer comprises gravel and cobbles with grain size based on the literature [60,61].
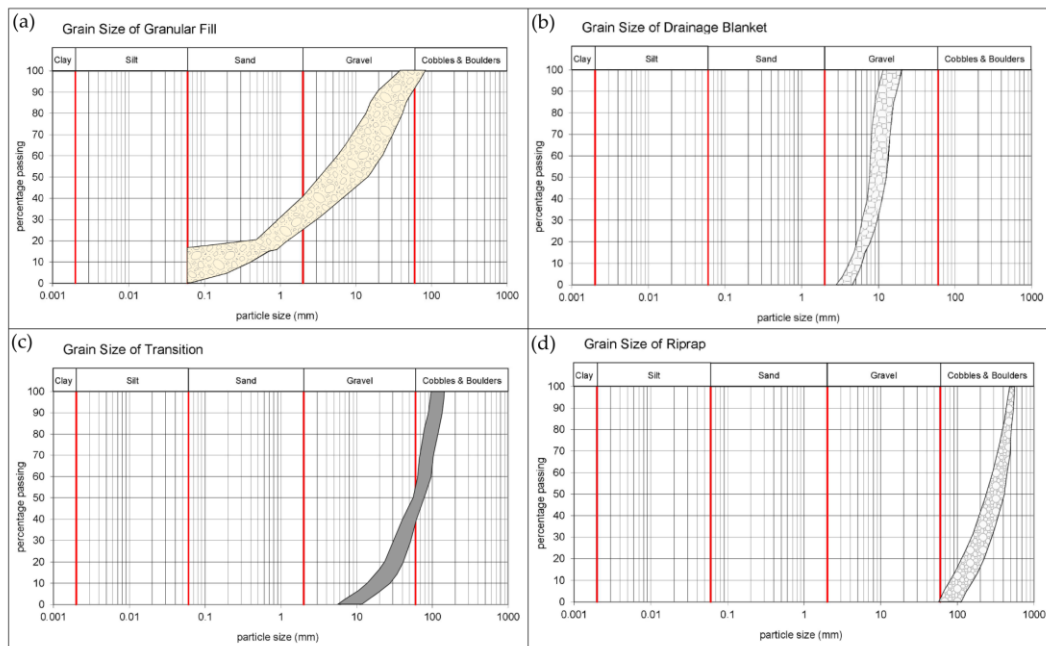

Figure 10. Grain size distribution of the dam embankment materials. (**a**) Granular fill consists of silty sandy gravel; (**b**) drainage blanket consists of uniform gravel; (**c**) transition layer comprises gravel and cobbles; (**d**) riprap consists of cobbles and boulders. The red lines represent the boundaries between the grain size classes.

4.3.2. Seepage and Filtration

An accurate seepage analysis was performed to estimate (i) the phreatic surface and the pore-pressures within embankment and foundations, taking into account the presence of the plastic concrete core; (ii) the hydraulic exit gradients and/or uplift pressures at the toe of the dam embankment; (iii) the flow discharge through the dam body and soil/rock foundations [78,79].

The following cases were examined:

- Initial steady state: Long term steady-state conditions with the reservoir at its normal retention level (full supply level—FSL) and the tail water at the ground surface;

- Transient analysis: Drawdown from normal retention level (FSL) to the lowest draw down level;
- Post-drawdown stability: Multiple time step stability analysis after drawdown.

An allowable value of the exit gradient equal to 0.25 was imposed.

The analyses were carried out for two representative sections: (i) the first section (case a) corresponding to the maximum height of the dam embankment (8 m) where the dam shoulders lay on the 5 m thick alluvial deposit (ALL); (ii) the second section (case b) corresponding to the maximum height of the spillway (5 m) resting on the 2 m thick alluvial deposit (ALL).

Based on the field investigations and the laboratory soil testing, the foundation soils were modelled with a three-layer soil profile: the alluvial deposit (ALL) covering Conglomerate (CG) followed by Marl (M).

The results of seepage analyses under steady seepage conditions are summarized in Table 3. For each case examined, the maximum flow and maximum exit gradient obtained are reported. The values obtained are lower than the allowable value of the exit gradient (0.25). Therefore, all the cases examined are satisfied with regard to the "heave" at the toe of the embankment.

Table 3. Results of the seepage analyses. Case (a) embankment at maximum height; case (b) spillway at maximum height.

Case	Dam Elevations (m a.s.l.)			Maximum Discharge (m³/s/m)	Maximum Vertical Exit Gradient
	Crest	Toe	Reservoir		
(a) Embankment at Maximum Height	371.60	363.85	368.50	2.6 E-005	0.19
(b) Spillway at Maximum Height	368.50	363.85	368.50	7 E-006	0.10

Regarding the stability of the upstream embankment during rapid drawdown, for the embankment (case a) the safety factor drops below 1.76 at the early stage of the drawdown process and increases up nearly 1.85 when the pore-water pressure in the embankment dissipates with time. For the spillway (case b) the safety factor drops below 1.6 at the early stage and then increases up nearly 1.7.

4.3.3. Slope Stability

Stability calculations were carried out by computing safety factors for the most severe load cases and considering both the static and seismic load conditions. The seismic design, carried out by means of the simplified pseudo-static method [72], considered the maximum credible earthquake (MCE) and the operating basis earthquake (OBE) [73]. According to Shedlocket al. [70], a peak ground acceleration of 1.6 was considered for the OBE analysis and 2.4 m/sec² for MCE analysis. Two cases (a, b) were considered, the same ones analyzed in the seepage analysis. The characteristic values of geotechnical parameters, derived from field and laboratory test results and summarized in Table 2, were converted to design values by dividing by the partial factor (γ_M) [55].

Load cases, side of the dam, reservoir conditions, and seismic coefficients k_h, and k_v [80,81] considered are listed in Table 4. In the same table, the minimum safety factors required (F_s) [56,73] and the minimum safety factors obtained (F) for each case examined are presented.

Table 4. Results of stability analysis: case (a) embankment at maximum height; case (b) spillway at maximum height.

Load Case	Side of the Dam	Reservoir Level [m a.s.l.]	k_h	k_v	F_s	F (Case "a")	F (Case "b")
EoC: End of Construction	Upstream	Empty	0	0	1.3	1.50	1.79
	Downstream	Empty	0	0	1.3	1.53	1.40
FSL: Full supply level	Upstream	368.50	0	0	1.3	1.45	1.45
MWL: Maximum Water Level—Extreme Case	Upstream	370.50	0	0	1.1	1.43	1.42
RDD: Rapid Drawdown	Upstream	Empty with water in the embankment	0	0	1.1	1.15	1.17
OBE: Operating Basis Earthquake	Upstream	Empty	0.04	−0.02	1.3	1.33	1.61
	Downstream	Empty	0.04	−0.02	1.3	1.38	1.40
OBE + Water Level at FSL	Upstream	140.00	0.04	−0.02	1.1	1.19	1.19
MCE: Maximum Credible Earthquake	Upstream	Empty	0.07	−0.035	1.0	1.25	1.49
	Downstream	Empty	0.07	−0.035	1.0	1.27	1.21

Based on the results, it was decided to set the shoulders slope to 1/2.2 (vertical/horizontal) and to excavate the alluvial deposit (ALL) to a maximum depth of approximately 4 m to remove any loose or old backfill materials. It was also planned to carry out upstream and downstream fillings to regularize the soil profile.

5. Discussion

5.1. Final Choice of the Dam Site

The geological, hydrogeological, and geotechnical studies together with the results of site investigations allowed us to choose the most appropriate area for IBRI 14 Recharge Dam and to define the nature, geometry, and consistency of the materials available.

To maximize recharge efficiency, the dam was positioned close to the narrowing of the wide floodplain of the Wadi Sulayf, downstream to the confluence between Wadi Lusayl and Wadi Manqas. The choice was guided by the following main aspects:

- Hydrological aspects: The potential aquifer storage is estimated to be about 1,300,000 m^3 [82].
- Geological survey results: (i) Presence of an alluvial body (sandy gravel, ~10 m thick) with medium–high permeability; (ii) occurrence of fractured sedimentary hard rock (Conglomerates, 5–12 m thick) with water circulation through fractures; (iii) emergence of bedrock at morphological thresholds, where the valley narrows and enhances aquifer flow concentration, as evidenced by agricultural activities and settlements; (iv) sedimentary rocks is less fractured and virtually waterproof (aquicludes).
- Hydrogeological setting: The water table is often located within the fractured rock mass.
- Hydrological function of the dam: Capable of collecting water from flash floods that occur in wadi systems in arid areas, such as Wadi Sulayf, in order to augment limited water resources [16]
- Socio-economic aspect: The selected location ensures greater benefits for many of the farms in the village of Sulayf than other studied sites.

5.2. Cross Section of the Recharge Dam System

The aim of recharge dams is to increase flood flow infiltration and thus increase the groundwater resources. The general criteria focus on the construction of small and relatively inexpensive dams that could increase the recharging mechanism of aquifers according to morphological and geological settings. Recharge dams temporarily stop the flood flow and slowly release it toward the recharge zone [13,38,83].

In the Ibri Project, the maximum possible contact with the absorption surface is guaranteed, both into the reservoir and downstream. The conceptual cross section is shown in Figure 11. Better absorption efficiency is achieved with a wide spillway, which allows the water flow to be distributed downstream into a wide stilling basin. Both the spillway and the stilling basin are constructed with gabions. The dam's effect slows the flow downstream, improving absorption in the riverbed.
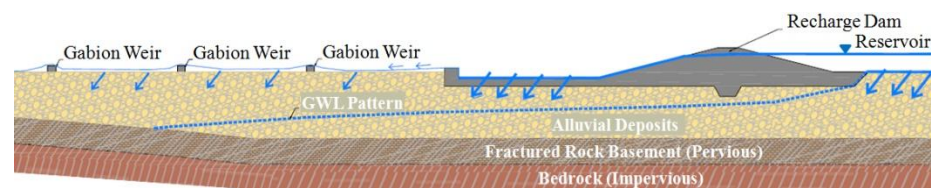

Figure 11. Conceptual cross section of IBRI 14 Recharge Dam. The light blue dotted line indicates the groundwater level (GWL) pattern, while the light blue arrows indicate the infiltration path.

The most effective infiltration is represented by the low-flow wadi bed downstream of the dam, which is not affected by silting and presents the most statistically efficient area suitable for the absorption. Therefore, the goal is to slow down the maximum water flowing downstream of the dam to increase the contact with gravelly deposits. This was possible through the correct dimensioning of spillway and bottom outlets.

Downstream of the dam, four small gabion weirs were provided to increase the permanence and contact of flow into the wadi bed. These weirs, with a height not exceeding 1.0–1.5 m, were strategically positioned near thresholds or narrow sections of the wadi. They reduce the stream gradient and, consequently, the flow speed and contribute to the development of calm areas and increase infiltration.

5.3. Description of the Dam

The detailed design of the IBRI 14 Dam was approved by MRMWR on December 2014. The complex of the IBRI 14 Recharge Dam includes (Figure 12) (i) the dam structure and related discharge works (spillway, intake tower, and two bottom outlets); (ii) the regularization of the ground level downstream the spillway; (iii) four weirs downstream.

The embankment has a rounded shape with a total length of about 3200 m to account for the land use of the area, with plenty of farms on the right side of the dam.

The main features of the dam are exposed in Table 5. The Height/Surface Curve determined based on the literature criteria [51,54] is shown in the right corner of Figure 12, while Figure 13 shows the typical sections of IBRI 14 Dam. The dam consists of an 8 m high rockfill embankment with an impervious core made of plastic concrete and a gabion spillway. A geotextile is interposed between the rockfill embankment and the gabions. At the downstream toe of the dam, a 1.0 m thick drainage blanket is located. A drainpipe collects the drainage water to the stilling basin. The slopes are protected upstream and downstream by a dumped riprap.

The grain size distribution of each part of the embankment is as follows: (i) silty sandy gravel for the granular fill of the embankment; (ii) uniform gravel for the drainage blanket; (iii) cobbles for the riprap; (iv) gravel and cobbles for the transition layer.

Rockfill dams are economical due to the large quantities of rock available from required excavations and/or nearby borrow sources, the ability to construct during wet and dry weather, and the ability to realize an impervious core with simultaneous placement of rockfill [53].

Based on the literature criteria [51] the crest has a width of 4 m along the higher sections and is 2 m wide in the other parts. The shoulders slope is 1/2.2 (V/H) upstream and downstream.

A typical section of the embankment varies depending on the crest width and/or as a function of particular elements to be executed such as the plastic concrete core wall, cut-off walls, and ditch, as illustrated in Figure 13. The embankment reaches its maximum height (8 m) at Section 21, while the spillway's at Section 24 (5 m).

To prevent water leakage through the dam embankment and to ensure safety against piping, an impervious plastic concrete core [78] is envisaged from Section 10 to Section 31 (Figure 12) where the embankment is higher than 4.5 m. The plastic concrete core is connected to the foundation through a concrete basement from Section 20 to Section 22 (Figure 12) and, in correspondence of the spillway, the impervious core extends up to 2 m below the embankment with a plastic concrete cut-off. Plastic concrete is thought to be less brittle than conventional concrete, and its stiffness is more compatible with the surrounding soils. [78]. Moreover, when the slurry wall is located through the crest of the dam, which tends to be the more common location when modifying a dam, it has the significant advantage of minimizing both foundation and embankment seepage [78].

The lack of fine-grained materials in the reservoir area excluded the possibility of a zoned dam and led to the choice of an artificial waterproof device for the dam seal. Based on SERING International experience and the literature data [4,18,21], we opted for a plastic concrete core and cut-off, aiming to achieve the best solution in terms of hydraulic watertight and construction feasibility of the system.
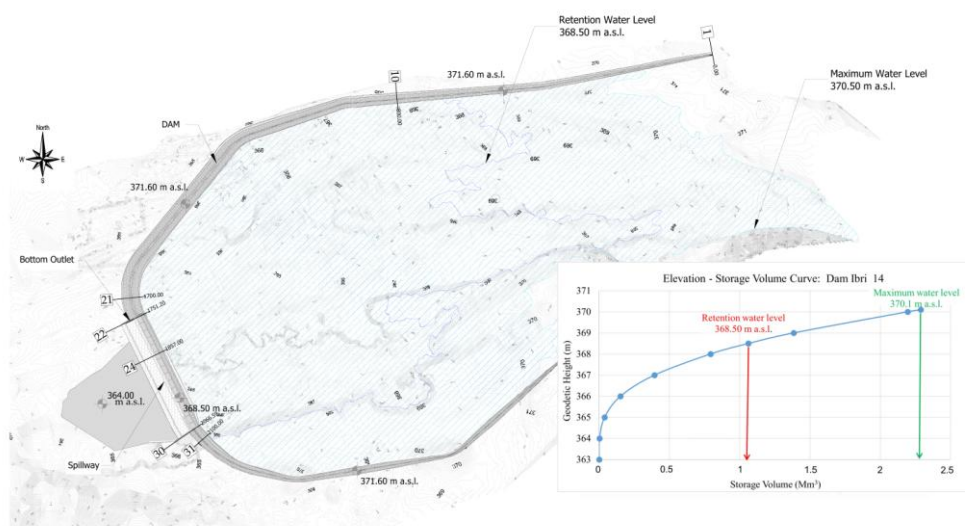

Figure 12. IBRI 14 Dam plan and height/surface. Elevation data are based on a detailed topographic survey carried out using a total station provided by SERING International.

Table 5. Main features of the dam.

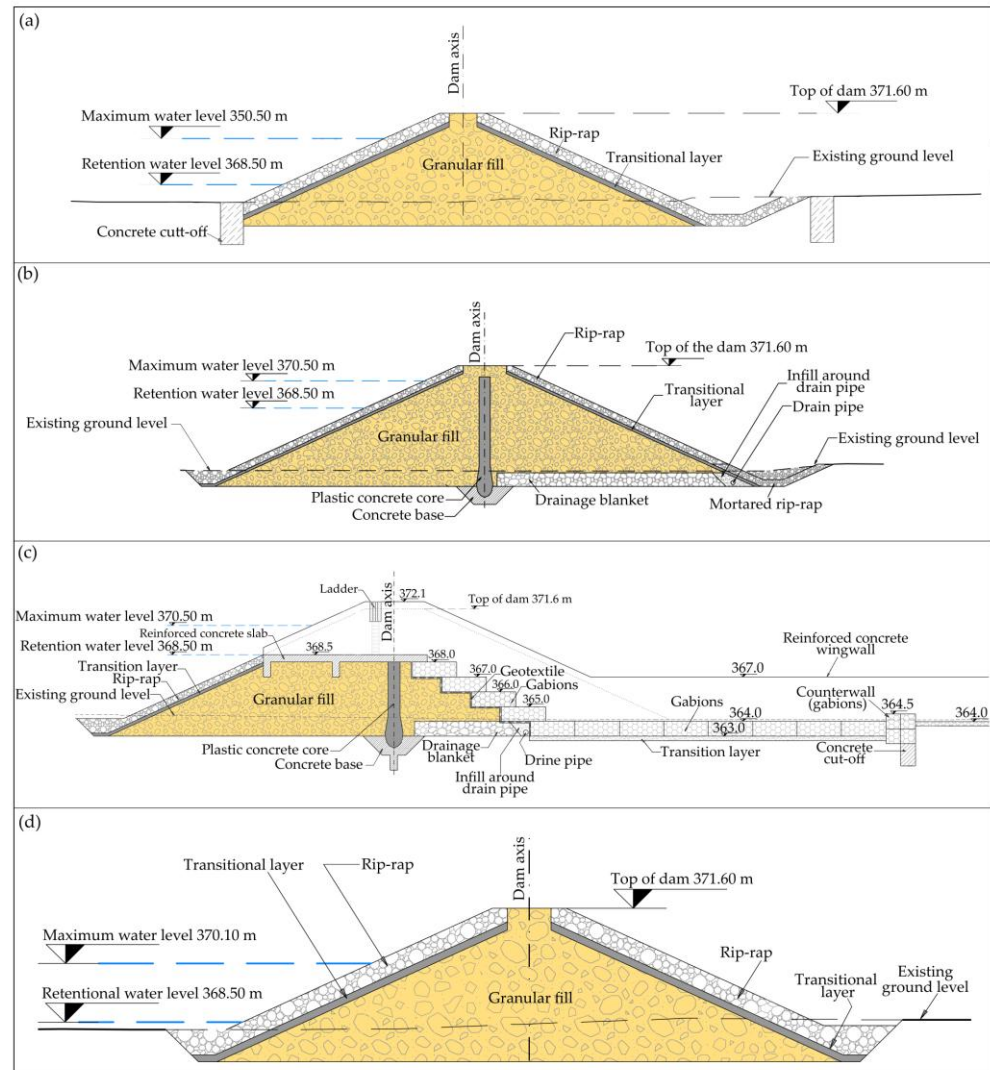| Maximum Dam Height H (m)	Alignment Length (m)	Maximum Water Level RWL (m a.s.l.)	Retention Water Level MWL (m a.s.l.)	Dam Crest Level (m a.s.l.)	Freeboard (m)	Crest Width (m)	Total Volume of the Dam (m³)
7.7	3192	368.50	368.50	371.60	1.5	2.0–4.0	192,678

Figure 13. Typical sections of the dam: (**a**) Type 1 between Section 1 and Section 10; (**b**) Type 2 between Section 10 and Section 22 and between Section 30 and Section 31; (**c**) spillway between Section 22 and Section 30; (**d**) type 4 between Section 31 and Section 43.

Another key aspect of the project was the positioning of the drainage blanket downstream near the base of the plastic concrete core to immediately intercept any leaks and help prevent piping problems.

The foundation soils are suitable for construction after removal of the top layer of the alluvial deposit (ALL).

An ungated gabion spillway, 313 m wide and designed for a maximum flow of 1510 m^3/s [74], followed by a stilling basin, is planned between Section 22 and Section 30 (Figure 12). The spillway, extending as far as the stilling basin, is built with gabions 3 m long and a superposition of 1 m, laying on geotextile (Figure 13c). The spillway section is completed by a rockfill embankment with an impervious plastic concrete core which extends up to 2.3 m below the embankment with a plastic concrete cut-off. The spillway crest, a horizontal inlet (El. 368.50 m a.s.l.), is composed of a flat concrete slab. The drainage blanket at the downstream toe of the dam and a concrete cut-off at the end of the stilling basin ensure stability against sliding and seepage.

A stilling basin 21 m long spreads the flow in the natural wadi (Figure 12). A gabions layer placed inside the stilling basin and resting on a transition layer prevents damage

from degradation or from scour (Figure 13c); a final gabion sill is provided, followed by a downstream apron composed of riprap.

The dam is equipped with two bottom outlets (service and emergency), designed for a maximum flow of 0.95 m³/s [75] and located inside the water intake tower. Each outlet is composed of a circular steel pipe ⌀ 600 mm running below the dam embankment and is regulated by penstock gates. A walkway bridge connects the intake tower with the crest of the dam for operation and maintenance.

According to the outcomes of the hydrogeological studies, the construction of four minor dams (weirs) made of granular fill and gabions is envisaged to improve ground-water recharge. The typical section is shown in Figure 14. The weirs are positioned at distances from the spillway of 950 m, 200 m, 2500 m, and 2800 m, respectively, on the base of the conceptual cross section of Figure 11.
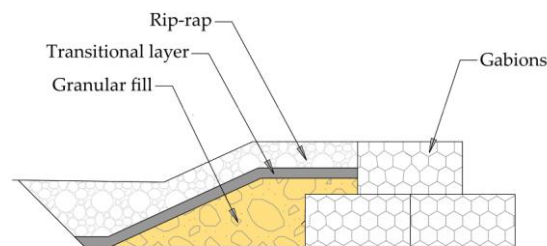

Figure 14. Typical section of a weir.

Recharge rockfill dams, with gabion and spillway similar to the IBRI14 Dam, have been built in Oman, among which several are reported in the technical literature and official documentation [3,4,13,17–19,21,22,84].

Unlike the recharge rockfill dams built in Oman, in the IBRI 14 Dam there is the simultaneous presence of an impervious plastic concrete core that extends up to 2 m below the embankment with a plastic concrete cut-off and of an ungated gabion spillway followed by a gabion stilling basin to dissipate the excess hydro-mechanical energy, the latter distributing the flow in the natural wadi.

Furthermore, all parts of the dam, except the waterproof structure, are made of alluvial materials from the wadi bed.

The monitoring programme envisaged in the project, partially completed, included a topographic survey with geodetic points installed on the dam surface; water level measurements with a level gauge; piezometric monitoring with standpipe piezometers; and monitoring of the sedimentation process in the basin with rows of sediment pegs. Dam monitoring, together with the installation of piezometers and monitoring of the wells downstream of the dam, is a fundamental aspect for assessing the hydrogeological response and the full functionality of the recharge dams over the years.

5.4. Main Conclusions of On-Site Investigations and Engineering Consequences

The results of the geological and geotechnical surveys and investigation allowed us to define the soil–structure interaction at Section 21 (Figure 15a) and at Section 24 (Figure 15b) corresponding to the maximum height of the dam and spillway, respectively. The geotechnical investigations confirmed that the dam's foundation is composed of alluvial deposit (ALL) covering Conglomerate (CG), Marl (M), and Limestone (L) as bedrock. The water table is uniformly distributed across the wadi bed.
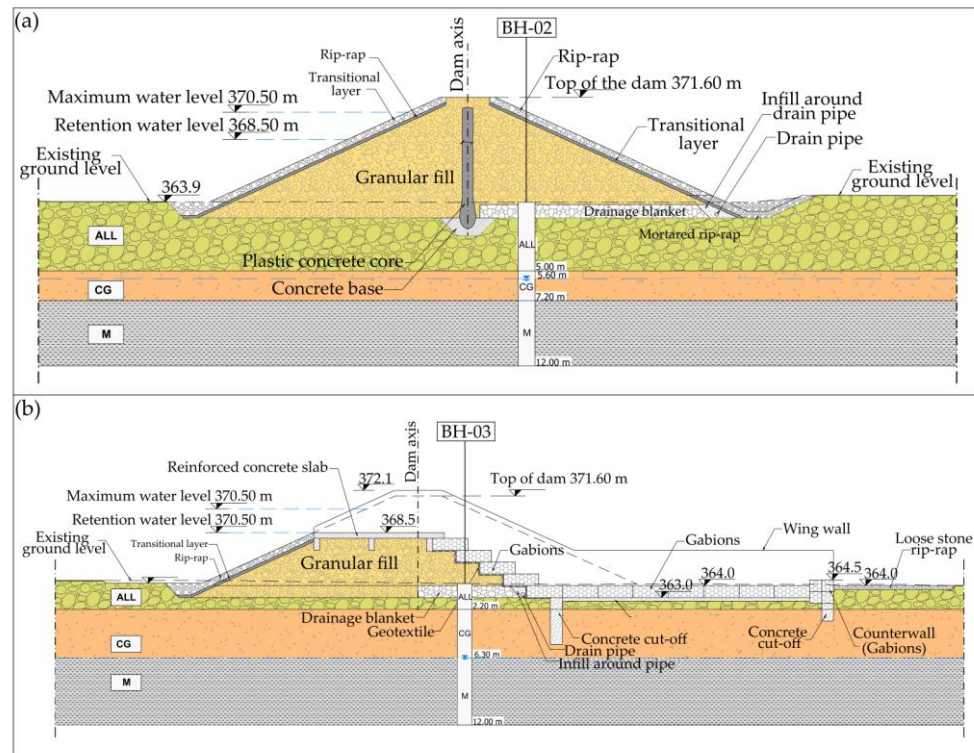
Figure 15. (**a**) Soil–structure interaction at Section 21; (**b**) soil–structure interaction at Section 24.

Overall, foundation soils and construction materials show appropriate physical and mechanical properties.

The foundation soils were poorly compressible and characterized by medium-to-high mechanical parameter values. Furthermore, it was observed that the values obtained from the in situ and laboratory tests agreed well with general mechanical characteristics collected from SERING International experience in Oman on similar soils.

At the time of the investigation, there was plenty of alluvial material within the wadi bed, suitable for use as granular fill for the construction of the various parts of the recharge dam, as they had an appropriate grain size distribution and excellent physical and mechanical properties after compaction. These results were also supported by the checks carried out during the supervision phase, successively illustrated. Moreover, the good performance of the embankment sections already completed after two exceptional flood events during the final phase of the construction works confirm the project validity, as explained below in paragraph about the flood events. Furthermore, as a consequence of foundation excavation, large amounts of good-quality alluvial deposits would have been excavated for use. Transitions and drains could be obtained by processing the alluvial deposits.

Based on boreholes and trial pits stratigraphy, the available material volume was estimated at approximately 1,000,000 m³. The position of the quarry area within the reservoir also guaranteed an increase in the useful volume of the reservoir.

5.5. Qualitative Analysis of Seepage Modelling and Stability Calculations Results

Regarding the seepage analysis performed by SEEP/W (GEO-SLOPE International Ltd., Calgary, Canada, v. 2015 commercial product, https://www.adalta.it/geostudio/#SLOPEW) [63], as shown in Figure 16 where the water total head is highlighted in colour, the flow paths (green lines) cross the equipotential lines at right angles and terminate against the drainage blanket, confirming the validity of the design choices and the analysis results.
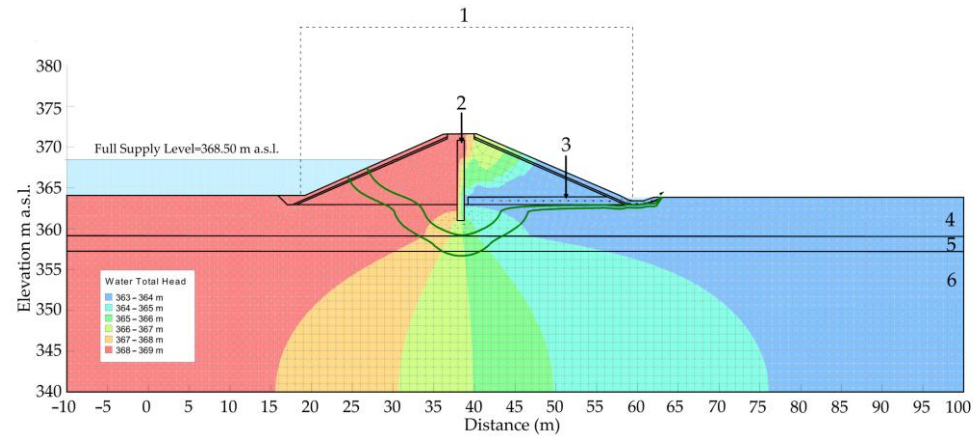
Figure 16. Seepage analysis calculated for the maximum height of the dam embankment. Total head contour at long term steady-state conditions. Green lines represent the flow path. (1) Dam embankment; (2) impervious plastic core; (3) drainage blanket; (4) alluvial deposit (ALL); (5) Conglomerate (CG); (6) Marl (M).

The maximum discharge, much less than 1 l/s, is very low.

The safety factor during the drawdown process, taking into account the filtration process in the upstream embankment, is high even after the completion of the first phase (5 days), further increasing in the next phase when the pore-water pressure in the embankment dissipated with time, confirming the validity of the materials used in this critical portion of the dam (upstream embankment) and of the design scheme.

Regarding the stability calculations, in all conditions examined, the safety factor F is satisfied and adequate (Table 4). The lowest value was obtained for the RDD load case (F = 1.17), the most critical condition for a dam, followed by the OBE + Water Level at FSL load case (F = 1.19), both slightly above the minimum safety factors required (Fs = 1.1). Values significantly higher than the prescribed minimums were obtained in the other cases examined, for both sides of the dam, in both static and seismic conditions.

The results of the seepage and stability calculations demonstrated the soundness of the design choices in terms of the structure's geometry (position of the various parts of the dam body, shoulders slope, position of the foundation level, etc.), which also allowed the thickness of the alluvial layer on which the dam rests to be kept to a minimum. These choices also had a positive economic impact on the cost of the project.

5.6. Supervision Phase

The construction of the dam embankment began on 17 October 2018 with the supervision of SERING International and was completed on 16 April 2020.

5.6.1. Materials Tests

During the construction, particular attention was paid to material controls. Several checks were carried out on reinforced concrete structures and on the embankment materials, such as layer thickness, degree of compaction, and permeability coefficient.

The construction of the first layers of the dam embankment was used to confirm the project specifications of the materials sourced from the reservoir. The tests primarily concerned the granular fill and included determining field density using the sand cone method [76] and permeability inside pits [42]. Moreover, sieve analyses [44] and Proctor tests [45] were performed in the laboratory.

In the initial phase the field test results on granular fill did not comply with the project requirements; the particle size distribution, indeed, fell outside the design range, causing slightly finer results (Figure 17a). The in situ coefficient of permeability k was found

to be lower by at least an order of magnitude (about 10^{-5} m/s) (Figure 17c) compared to the prescribed limit ($k = 10^{-3}$ m/s), while the on-site dry unit weight values were significantly higher than those required (Figure 17b).
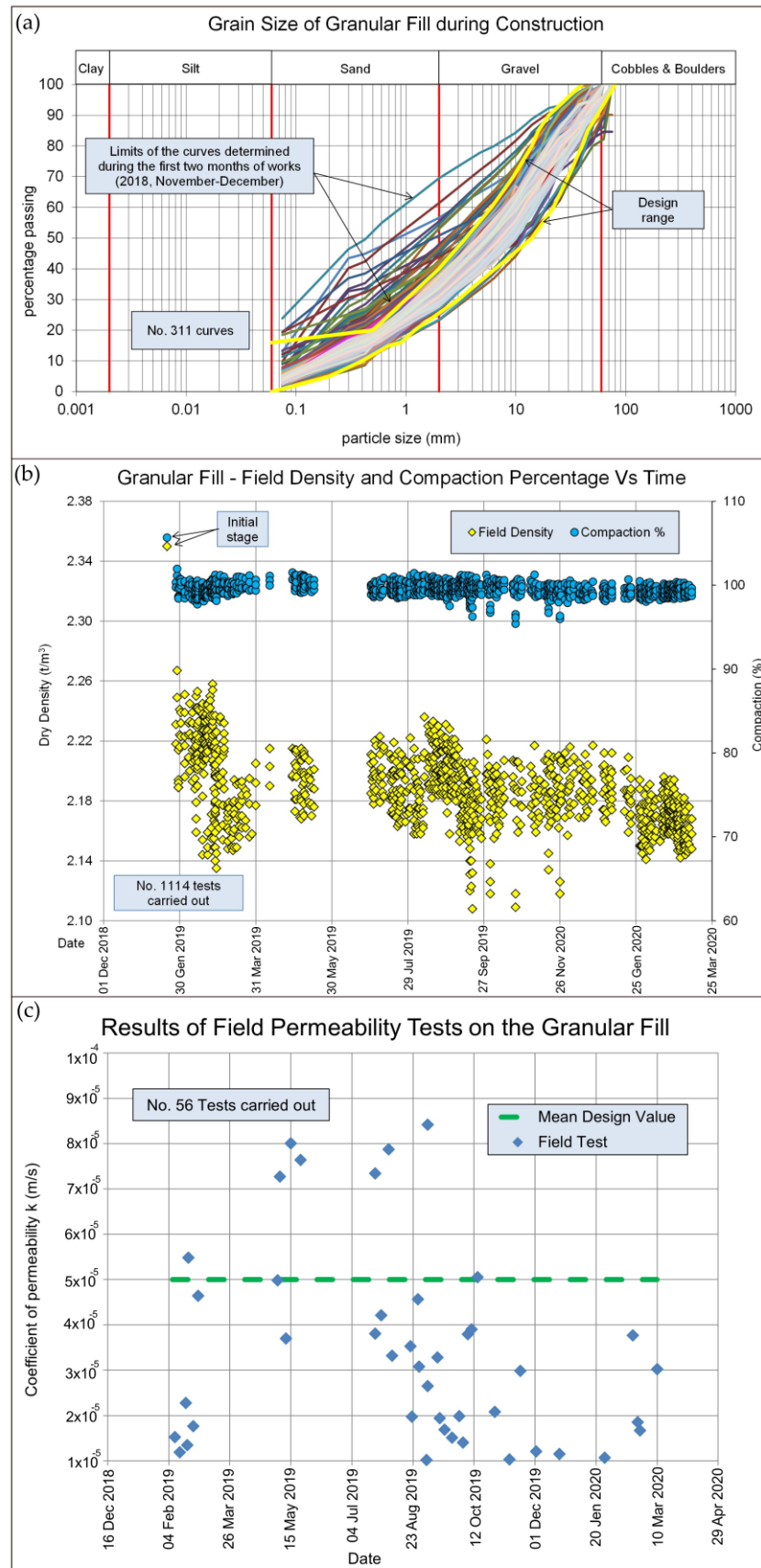
Figure 17. Results of the on-site checks on granular fill. (**a**) grain size distribution; (**b**) field density and compaction percentage; (**c**) results of the on-site permeability test on granular fill.

Improved material selection methods of the granular fill and screening systems, as well as the compaction in 40 cm thick layers, quickly allowed the project to meet specifications regarding grain size distribution and dry unit weight. Since January 2019, the grain size has always been within the design range, except for slight deviations, as can be seen from the results of 311 determinations shown in Figure 17a. The dry unit weight values (1114 tests) were always within the specification limits, except in a few cases (Figure 17b).

Regarding permeability, in the absence of significant improvements, SERING International repeated seepage analyses, assuming an average value of $k = 5 \times 10^{-5}$ m/s m/s for the granular fill instead of the design value of $k = 1 \times 10^{-5}$ m/s. Essentially, the maximum vertical exit gradient remained unchanged, while the maximum discharge and the safety factor during rapid drawdown was reduced (albeit slightly), while still maintaining the required safety conditions. Lastly, the average value of $k = 5 \times 10^{-5}$ m/s was adopted. The obtained permeability values during on-site tests, distributed between 1.1×10^{-5} m/s and 8.4×10^{-5} m/s (Figure 17c), were considered acceptable.

During the construction works, checks on the particle size of the transition, the drainage blanket, and the riprap consistently yielded positive results. Checks were also carried out on the concrete of the impervious core and on the concrete and steel of the reinforced concrete structures, with consistently satisfactory results.

5.6.2. Flood Events

In the final phase of the construction works, two exceptional flood events occurred in the IBRI 14 Dam area.

The first event occurred on 8 December 2019, and was documented by SERING International (Figure 18a). A severe thunderstorm affected the area, with rainfall starting at 1:00 AM and continuing intermittently until 2:00 PM. On that day, the Ibri Weather Station, located about 6 km west downstream of the dam, recorded 87 mm of rainfall [85,86]. A maximum water depth of 1.5 m was measured within the dam reservoir, between Section 10 and Section 21 of the dam (see Figure 12 for sections position). The wadi flow entered the stilling basin section and submerged the whole spillway section including recently placed first row of gabion boxes. The benching work of Spillway downstream section for placing gabion boxes was partially damaged and rain cuts developed on the edges of granular fill with the effects visible in Figure 18b. On the right embankment, where construction was in progress, some parts close to Section 21 of the dam (see Figure 12 for sections position) were washed away by wadi flow. Conversely, on the trimming of the right side of embankment on both sides, no major rain cuts were observed and remained intact, as well as on the left side downstream of the embankment. No damage was found on the transition layer and loose riprap laid on the embankments, the walls/foundations of the spillway, and the bottom outlet and HDPE pipe fixed at the site.

The few damages observed, which could be expected from an inundation, were promptly repaired, and construction of the embankment continued, being completed in the first week of March 2020.

A second flood occurred on 22 March 2020. Although the Ibri Weather Station recorded a lower amount of rainfall (21 mm) [86] with respect to the event of 8 December 2019, intense precipitation in the upstream catchment produced a significant flood passing over the spillway (Figure 18c). No structural damage was observed except for small accumulations of debris and wood along the spillway and the stilling basin which were promptly removed, as documented in the photograph on 4 April 2020 (Figure 18d).

Figure 18. (**a**) Flood event of 8 December 2019; (**b**) the spillway after the flood event of 8 December 2019; (**c**) flood event of 22 March 2020 crossing the spillway; (**d**) the spillway on 4 April 2020.

After the end of the works, a new flood event occurred coinciding with the passage of cyclone Shaheen, which hit Oman on 4 October 2021. An inspection carried out by SER-ING International two weeks later highlighted the excellent Behaviour of the dam following the passage of the flood, which reached a height of 369.50 m a.s.l., one metre above the spillway slab. The embankment did not show any signs of distress. The spillway and the stilling basin showed no sign of movement, only a small accumulation of wood and pieces of palm trees in the stilling basin. Minor cracks were found in the spillway step covers since the concrete over the gabions was not reinforced concrete. No seepage was observed downstream of the dam. Minor side erosion was observed on the weirs. Ultimately, the water from the first significant flood after the end of construction was discharged from the dam as planned and designed with no evidence of distress that could affect the safety of the dam.

This demonstrates that, given the geotechnical and engineering considerations established during the design phase, the dam's structure has remained resilient to these extreme weather events throughout the various construction stages and into the subsequent operational phase. Indeed, similar extreme events have frequently resulted in significant damage to this type of engineering structure within the Sultanate of Oman [87,88] and neighbouring regions [89].

6. Conclusions

The present paper illustrates the study and work carried out by SERING International for the IBRI 14 Dam, designed to meet the growing water demand in Oman. The study defined site selection criteria, carried out geological and geotechnical investigations, and developed the dam's design according to Omani and international standards. Key aspects included the dam's geometry and zoning, seepage and filtration studies, and slope stability.

Several key factors, as studied through surveys and investigations, informed the choice of the dam site. Firstly, a potential aquifer accumulation of approximately 1,300,000 m³ was considered. Secondly, the presence of a medium–high permeability alluvial body overlying fractured Conglomerates, with water circulation in the fractures, was reconstructed. Finally, a crucial aspect for the choice of the dam site location is represented by the outcropping of a rocky substrate constituting a morphological threshold west to the study area.

The Wadi Sulayf, where the IBRI 14 Dam was positioned, is indeed occupied by a very dense alluvial deposit, sequentially covering Conglomerates, Marls, and Limestones. In this study a water table uniformly present across the wadi bed was recognized within the four boreholes. Moreover, the presence of plenty of alluvial materials within the wadi bed, suitable for use as granular fill both for the construction of the shoulders and the riprap of the project dam, was described. Foundation soils and construction materials showed appropriate physical and mechanical properties.

To enhance floodwater infiltration, the design maximized contact with the absorption surface and included a wide spillway that distributes the water flow downstream into a large stilling basin. The effect of the dam is to slow the flow downstream, improving the absorption in the riverbed. Groundwater recharge was further improved by four gabion weirs placed in the wadi bed near natural thresholds.

The IBRI 14 dam consists of an 8 m high rockfill embankment made of granular fill, with an impervious plastic concrete core, an ungated gabion spillway, and two bottom outlets (Figure 19a,b).

Figure 19. (**a**) The spillway of the IBRI14 Dam and the intake tower on August 2020; (**b**) the right embankment on October 2021.

During construction, initial granular fill tests did not meet requirements, but improved material selection, screening, and 40 cm compaction layers ensured compliance. Seepage checks, using an updated on-site permeability value of 5×10^{-5} m/s, proved acceptable. In the final stage, the dam withstood two exceptional floods without significant damage, unlike the nearby town of Ibri.

It is recommended that future designs of similar dams take due account of the choice and laying of dam body materials, to ensure the dam's safety in the event of flooding, which could also occur during construction works, as was the case with the Ibri 14 dam.

Beyond its hydraulic function, the IBRI 14 Dam has also become a tourist attraction, complementing Ibri Castle and the nearby UNESCO World Heritage sites of Bat, Al-Khutm, and Al-Ayn [4].

References

1. Kwarteng, A.Y.; Dorvlo, A.S.; Vijaya Kumara, G.T. Analysis of a 27 Year Rainfall Data (1977–2003) in the Sultanate of Oman. *Int. J. Climatol.* **2009**, *29*, 605–617. https://doi.org/10.1002/joc.1727.

2. Al-Ajmi, D.N. Climate Aridity: The Sultanate of Oman as a Case Study. *Int. J. Earth Sci. Geol*. **2018**, *1*, 1–3. https://doi.org/10.18689/ijeg-1000101.

3. Abdalla, O.A.; Al-Rawahi, A.S. Groundwater recharge dams in arid areas as tools for aquifer replenishment and mitigating seawater intrusion: Example of AlKhod, Oman. *Environ. Earth Sci.* **2013**, *69*, 1951–1962. https://doi.org/10.1007/S12665-012-2028-X.

4. Sultanate of Oman, Ministry of Regional Municipalities & Water Resources (MRMWR). Water Resources in the Sultanate of Oman. In Proceedings of the Occasion of the Expo Zaragoza Water and Sustainable Development, Zaragoza, Spain, 14 June–14 September 2008.

5. McDonnell, R. Groundwater use and policies in Oman. *IWMI Proj. Rep.* **2016**, *14*, 32.

6. MRMEWR (Ministry of Regional Municipalities, Environment and Water Resources). The Aflaj Irrigation System of Oman. Nomination to the UNESCO World Heritage List. MRMEWR, Directorate General of Water Resources Affairs, Sultanate of Oman. 2006. Available online: https://whc.unesco.org/en/list/1207/ (accessed on 18 November 2022).

7. Al Amri, S.; Al Ghafri, A.; Abd Rahman, N. Water Management of Falaj Al Khatmain in Sultanate of Oman. *J. Earth Sci. Eng.* **2014**, *4*, 127–133.

8.   Medomed, Aflaj Irrigation System, Oman. Available online: https://medomed.org/featured_item/the-cultural-landscape-of-aflaj-irrigation-system-oman/ (accessed on 1 August 2025).

9.   Al Ghafri, A. Overview about the Aflaj of Oman. In Proceeding of the International Symposium of Khattaras and Aflaj, Era-chidiya, Morocco, 9 October 2018; Volume 9, pp. 1–22.

10.   Sultanate of Oman; Ministry of Regional Municipalities & Water Resources (MRMWR). *Aflaj Oman in the World Heritage List*; MRMWR Department of Awareness and Information. Muscat, Sultanate of Oman, 2008.

11.   Ministry of Agriculture and Fisheries, Oman. Available online: https://www.ea.gov.om/en/knowledge-center/authority-direc-tory/government-organizations/ministry-of-agriculture-and-forest/ (accessed on 6 October 2025).

12.   Al Mamary, S.A. Effect of climate change on Aflaj in the Sultanate of Oman. In Proceeding of the Oman's International Confer-ence on Water Engineering & Management of Water Resources, Muscat, Oman, 9–11 November 2021; pp. 131–150.

13.   UNESCO. International Association of Hydrogeologists. Commission on Managed Aquifer Recharge. Gale I. Strategies for Man-aged Aquifer Recharge (MAR) in Semi-Arid Areas; 2005; IHP/2005/GW/MAR, UY/2005/SC/PHI/PI/1. Available online: https://unesdoc.unesco.org/search/04ff1fd6-f359-4b0f-a8f7-28a9c73ddd06 (accessed on 20 November 2022).

14.   International Association of Hydrogeologists Commission on Managing Aquifer Recharge (IAH-MAR). 2025. Available online: www.iah.org/recharge (accessed on 5 October 2025).

15.   Al-Battashi, M.B.; Ali, S.R. Groundwater Recharge Dam and Hydrogeology of Wadi Al-FulayJ, Wilayat Sur, Sultanate of Oman. In Proceedings of the Third Gulf Water Conference, Muscat, Oman, 8–13 March 1997; Volume 1, pp. 395–311.

16.   Al-Maktoumi, A.; Kacimov, A.; Al-Busaidi, H.; Al-Ismaily, S.; Kantoush, S.A.; Saber, M. Impact of Sedimentation of Recharge Dams on Water Resources Management: Overview from Oman. In Proceedings of the 9th International Conference in Flood Management: River Basin Disaster Resilience and Sustainability, Tsukuba, Japan, 18–22 February 2023.

17.   Al-Harthy, S. Al Khawd recharge dam preliminary conclusions on first years of operation. In Proceedings of the 2nd Interna-tional Symposium on Artificial Recharge of Ground Water, Orlando, FL, USA, 17–22 July 1995; pp. 188–197.

18.   Ministry of Water Resources (MWR); *Dams in the Sultanate of Oman*; Ministry of Water Resources (MWR): Al Khuwair, Oman, 1998.

19.   Bajjali, W. The effect of Hilti/Salahi Recharge Dam in Batineh Area, Sultanate of Oman on the Quality of Groundwater Using GIS. In Proceedings of the Twenty-Second Annual Esri International User Conference, San Diego, CA, USA, 8–12 July 2002.

20.   Al-Kindi, R.S. Assessment of Groundwater Recharge from the Dam of Wadi Al-Jizzi, Sultanate of Oman. 2004. Available online: https://scholarworks.uaeu.ac.ae/all_theses/367/ (accessed on 20 November 2022).

21.   Sultanate of Oman. Ministry of Regional Municipalities and Water Resources (MRMWR). *Dams in the Sultanate of Oman*; Sultan-ate of Oman: Muscat, Oman, 2010. (In Arabic)

22.   Al-Maktoumi, A.; Al-Saqri, S.; Faber, Z.; Al-Ismaily, S.; Kacimov, A.; Al Busaidi, H. Hydropedology and Water Resources Man-agement: Case Study OF Al-Khoud Recharge Dam. In Proceedings of the 11th Gulf Water Conference, Muscat, Oman, 20–22 October 2014; Sultan Qaboos University: Muscat, Oman, 2014.

23.   Google Earth. Available online: https://earth.google.com/web/ (accessed on 4 October 2025).

24.   Robertson, A.H.F.; Searle, M.P.; Ries, A.C. Introduction. In *The Geology and Tectonics of the Oman Region*; Robertson, A.H.F., Searle, M.P., Ries, A.C., Eds.; Geological Society, London, Special Publications: London, UK, 1990; Volume 49, pp. 11–18. https://doi.org/10.1016/0191-8141(91)90110-5.

25.   Rollinson, H.R.; Searle, M.P.; Abbasi, I.A.; Al-Lazki, A.I.; Al Kindi, M.H. Tectonic evolution of the Oman Mountains: An intro-duction. In *Tectonic Evolution of the Oman Mountains*; Rollinson, H.R., Searle, M.P., Abbasi, I.A., Al-Lazki, A., Al Kindi, M.H., Eds.; Geological Society, London, Special Publications: London, UK, 2014; Volume 392, pp. 1–7. https://doi.org/10.1144/SP392.1.

26.   Glennie, K.W.; Boeuf, M.G.A.; Hughes, C.W.; Moody, S.M.; Pilaar, W.F.H.; Reinhardt, B.M. Geology of the Oman Mountains. *Verh. K. Ned. Geol. Mijnbouwkd. Genoot*. **1974**, 31, 423. https://doi.org/10.1016/0040-1951(77)90059-2.

27.   Rabu, D. Stratigraphy and Structure of the Oman Mountains. In *Document du Bureau de Recherches Géologiques et Minières 221*; BRGM: Orléans, France, 1993.

28.   Baud, A.; Béchennec, F.; Cordey, F.; Krystyn, L.; Le Métour, J.; Marcoux, J.; Maury, R.; Richoz, S. Permo-Triassic Deposits: From the Platform to the Basin and Seamounts. In *Field Guidebook, Excursion A01*, *Proceedings of the Conference on the Geology of Oman, Muscat, Oman, 8–11 January*; 2001; Volume 1, pp. 1–54. Available online: https://www.researchgate.net/publication/236624812 (accessed on 20 August 2025).

29.   Blechschmidt, I.; Dumitrica, P.; Mater, A.; Krystyn, L.; Peters, T. Stratigraphic architecture of the northern Oman continental margin—Mesozoic Hamrat Duru Group, Hawasina complex, Oman. *GeoArabia* **2004**, 9, 81–132. https://doi.org/10.2113/geoara-bia090281.

30. Glennie, K.W. *The Geology of the Oman Mountains: An Outline of their Origin*, 2nd ed.; Scientific Press: Bucks, UK, 2005.

31. Cooper, D.J. Structural architecture of a thin-skinned imbricate fan: Evidence from Mesozoic deepwater sediments in the Jabal Wahrah area of the central Oman Mountains. *GeoArabia* **2011**, *16*, 17–42. https://doi.org/10.2113/geoarabia160117.

32. Searle, M.P. *Geology of the Oman Mountains, Eastern Arabia*; Springer: Cham, Switzerland, 2019; p. 478. https://doi.org/10.1007/978-3-030-18453-7.

33. Minoux, L.; Janjou, D. *Geological Map of Ibri, Sheet NF 40-2F Scale 1:100,000 with Explanatory Notes*; Directorate General of Minerals, Oman Ministry of Petroleum and Minerals: Muscat, Oman, 1986.

34. Searle, M.P. Structural geometry, style and timing of deformation in the Hawasina Window, Al Jabal al Akhdar and Saih Hatat culminations, Oman Mountains. *GeoArabia* **2007**, 12, 99–130. https://doi.org/10.2113/geoarabia120299.

35. QGIS Development Team QGIS Geographic Information System. Open Source Geospatial Foundation Project. Available online: https://qgis.org/project/visual-changelogs/visualchangelog330/ (accessed on 20 August 2025).

36. NASA Shuttle Radar Topography Mission (SRTM). Shuttle Radar Topography Mission (SRTM) Global. Distributed by OpenTopography. 2013. Available online: https://portal.opentopography.org/datasetMetadata?otCollectionID=OT.042013.4326.1 (accessed on 18 November 2022).

37. UNESCO. Water Security. 2025. Available online: https://www.unesco.org/en/water (accessed on 2 August 2025).

38. Dillon, P. Future management of aquifer recharge. *Hydrogeol. J.* **2005**, *13*, 313–316. https://doi.org/10.1007/S10040-004-0413-6.

39. Eslamian, S. *Handbook of Engineering Hydrology: Environmental Hydrology and Water Management*; CRC Press: Boca Raton, FL, USA, 2014; pp. 17–31. https://doi.org/10.1201/b16766.

40. *ASTM STP 984*; Rock Classification Systems for Engineering Purposes. American Society for Testing and Materials: Philadelphia, PA, USA, 1988; pp. 91–101.

41. *BS 1377-9*; Methods for Test for Soils for Civil Engineering Purposes. British Standards Institute: London, UK, 1990.

42. *BS 5930*; British Standard Methods of Practice for Site Investigation. British Standards Institute: London, UK, 1999.

43. *BS 6297*; Design and Installation of Small Sewage Treatment Works and Cesspools. British Standards Institution: London, UK, 1983.

44. *ASTM D422*; Test Designation. Standard Method for Particle Size Analysis of Soils. ASTM: Philadelphia, PA, USA, 1972.

45. *ASTM D1557*; Standard Test Methods for Laboratory Compacted Characteristics of Soil Using Standard Effort (2700 kNm/m^3). ASTM International: West Conshohocken, PA, USA, 2010.

46. ISRM. International Society for Rock Mechanics. Suggested methods for determining the uniaxial compressive strength and deformability of rock materials. Part 1. Suggested method for determining deformability of rock materials in uniaxial compression *Int. J. Rock Mech. Min. Sci. Geomech. Abstr.* **1979**, 16, 138–140. https://doi.org/10.1016/0148-9062(79)91450-5.

47. ISRM. Suggested method for determining point load strength. *Int. J. Rock Mech. Min. Sci.* **1985**, 22, 53–60. https://doi.org/10.1016/0148-9062(85)92327-7.

48. Sultanate of Oman; Ministry of Transport and Communications. Highway Design Standards. 2010. Available online: https://bookstation.org/book/sultanate-of-oman-highway-design-standards-2010-4973085 (accessed on 15 November 2022).

49. MRMWR (Ministry of Regional Municipalities, Environment and Water Resources). Sultanate of Oman. *Regulations for Crushers, Quarries and Transport of Sand from Coasts, Beaches and Wadis. Ministerial Decision No. (200/2000)*; 2000. Available online: https://www.ea.gov.om/media/1cvg1oq4/decisions1439217556.pdf (accessed on 18 August 2025)

50. Harr, M.E. *Groundwater and Seepage*; McGraw-Hill Book Company: New York, NY, USA, 1962.

51. United States Department of the Interior; Bureau of Reclamation (USBR). *Design of Small Dams*, 3rd ed.; A Water Resources Technical Publication; Govt. Printing Office: Washington, DC, USA, 1987.

52. U.S. Army Corps of Engineers. *Seepage Analysis and Control for Dams Engineer Manual EM 1110-2-1901*; U.S. Army Corps of Engineers: Washington, DC, USA, 1993.

53. U.S. Army Corps of Engineers. *Earth and Rock-Fill Dams. General Design and Construction Considerations; Engineer Manual EM 1110-2-2300*; U.S. Army Corps of Engineers: Washington, DC, USA, 1994.

54. U.S. Army Corps of Engineers. *Hydrologic Engineering Requirements for Reservoirs; Engineer Manual EM 1110-2-1420*; U.S. Army Corps of Engineers: Washington, DC, USA, 1997.

55. *EN 1997-1*; Eurocode 7: Geotechnical design. Part 1: General rules. CEN: Brussels, Belgium, 2004.

56. U.S. Army Corps of Engineers. *Slope Stability; Engineer Manual EM 1110-2-1902*; U.S. Army Corps of Engineers: Washington, DC, USA, 2003.

57. Terzaghi, K. *Theoretical Soil Mechanics*; John Wiley & Sons, Inc.: New York, NY, USA; London, UK, 1943. https://doi.org/10.1002/9780470172766.

58. Sherard, J.L.; Dunnigan, L.P.; Talbot, J.R. Basic properties of sand and gravel filters. *J. Geotech. Eng.* **1984**, *110*, 684–700. https://doi.org/10.1061/(ASCE)0733-9410(1984)110:6(684).

59. Sherard, J.L.; Dunnigan, L.P. Critical filters for impervious soils. *J. Geotech. Eng.* **1989**, *115*, 927–947. https://doi.org/10.1061/(ASCE)0733-9410(1989)115:7(927).

60. USDA (United States Department of Agriculture). *Riprap for Slope Protection Against Wave Action Technical Release*; USDA: Washington, DC, USA, 1983; Volume 69

61. Lagasse, P.F.; Clopper, P.E.; Zevenbergen, L.W.; Ruff, J.F. Riprap Design Criteria, Recommended Specifications, and Quality Control. In *National Cooperative Highway Research Program (NCHRP) Report 568*; Transportation Research Board: Washington, DC, USA, 2006.

62. Thieu, N.T.M.; Fredlund, M.D.; Fredlund, D.G.; Hung, V.Q. Seepage modeling in a saturated/unsaturated soil system. In Proceedings of the International Conference on Management of the Land and Water Resources, Hanoi, Vietnam, 20–22 October 2001; pp. 20–22.

63. Geo-Slope International Ltd. SEEP/W: Seepage Modeling with GeoStudio, 2015 [Computer Software]. Available online: https://www.adalta.it/geostudio/#SEEPW (accessed on 15 September 2015).

64. Kovács, G. *Seepage Hydraulics (Developments in Water Science; 10)*; Elsevier Science Publishers: Amsterdam, The Netherlands, 1981.

65. Aubertin, M.; Mbonimpa, M.; Bussière, B.; Chapuis, R.P. A Model to Predict the Water Retention Curve from Basic Geotechnical Properties. *Can. Geotechn. J.* **2003**, 40, 1104–1122. https://doi.org/10.1139/t03-054.

66. Harr, M.E. *Mechanics of Particulate Media*; McGraw-Hill: New York, NY, USA, 1977.

67. Cedergren, H.R. *Seepage, Drainage and Flow Nets*, 2nd ed.; Wiley: New York, NY, USA, 1977.

68. Geo-Slope International Ltd. SLOPE/W: Stability Modeling with GeoStudio, 2015 [Computer Software]. Available online: https://www.adalta.it/geostudio/#SLOPEW (accessed on 15 September 2015).

69. Morgenstern, N.R.U.; Price, V.E. The analysis of the stability of general slip surfaces. *Geotechnique* **1965**, *15*, 79–93. https://doi.org/10.1680/geot.1965.15.1.79.

70. Shedlock, K.M.; Giardini, D.; Grünthal, G.; Zhang, P. The GSHAP global seismic hazard map. *Seismol. Res. Lett.* **2000**, 71, 679–686. https://doi.org/10.1785/gssrl.71.6.679.

71. *EN 1998-1*; Eurocode 8: Design of Structures for Earthquake Resistance. Part 1: General Rules, Seismic Actions and Rules for Buildings. CEN: Brussels, Belgium, 2004.

72. *EN 1998-5*; Eurocode 8: Design of Structures for Earthquake Resistance. Part 5: Foundations, Retaining Structures and Geotechnical Aspects. CEN: Brussels, Belgium, 2004.

73. U.S. Army Corps of Engineers. *Earthquake Design and Evaluation for Civil Works Projects, ER 1110-2-1806*; U.S. Army Corps of Engineers: Washington, DC, USA, 1995.

74. U.S. Army Corps of Engineers. *Hydraulic Design of Spillways; Engineer Manual EM 1110-2-1603*; U.S. Army Corps of Engineers: Washington, DC, USA, 1990.

75. U.S. Army Corps of Engineers. *Hydraulic Design of Reservoir Outlet Works; Engineer Manual EM 1110-2-1602*; U.S. Army Corps of Engineers: Washington, DC, USA, 1980.

76. *ASTM D1556*; Standard Test Method for Density and Unit Weight of Soil in Place by the Sand Cone Method. ASTM International: West Conshohocken, PA, USA, 2000.

77. Terzaghi, H.; Peck, R.B.; Mesri, G. *Soil Mechanics in Engineering Practice*; Wiley-IEEE: Piscataway, NJ, USA, 1996; pp. 1–549.

78. Richards, K.; Doerge, B.; Pabst, M.; Hanneman, D.; O'Leary, T. *Evaluation and Monitoring of Seepage and Internal Erosion*; Leffel, S., Ed.; FEMA: Washington, DC, USA, 2015.

79. Adamo, N.; Al-Ansari, N.; Sissakian, V.; Laue, J.; Knutsson, S. Dam Safety Problems Related to Seepage. *J. Earth Sci. Geotech. Eng.* **2020**, *10*, 191–239. https://doi.org/10.47260/jesge/1113.

80. Newmark, N.M. Effects of earthquakes on dams and embankments. *Géotechnique* **1965**, *15*, 139–160. https://doi.org/10.1680/geot.1965.15.2.139.

81. Seed, H.B. Considerations in the earthquake-resistant design of earth and rockfill dams. *Géotechnique* **1979**, *29*, 215–263. https://doi.org/10.1680/geot.1979.29.3.215.

82. Paliaga, G.; Minetti L.; Pittaluga F.; Aquifer Recharging System in Oman: Ibri Area. Case Study for Locating Small Dams and weirs where the hydrogeology and morphology make benefits exceed costs. In Proceedings of the Conference IAH2015 Rome—42th International Association of Hydrogeologists Congress, Rome, Italy, 13–18 September 2015.

83. Standen, K.; Costa, L.R.D.; Monteiro, J.P. In-Channel Managed Aquifer Recharge: A Review of Current Development Worldwide and Future Potential in Europe; *Water* **2020,** *12, 3099.* https://doi.org/10.3390/w12113099.

84. Djuma, H.; Bruggeman, A.; Camera, C.; Marinos Eliades, M.; Kostarelos, K. The Impact of a Check Dam on Groundwater Recharge and Sedimentation in an Ephemeral Stream. *Water* **2017**, *9*, 813. https://doi.org/10.3390/w9100813.

85. Sultanate of Oman. National Centre for Statistics. Data Portal. Weather. 2022. Available online: https://data.gov.om/bixytwb/weather# (accessed on 20 August 2025).

86. Meteomanz. Available online: http://www.meteomanz.com (accessed on 23 August 2025).

87. Abdel-Fattah, M.; Kantoush, S.; Saber, M.; Sumi, T. Hydrological modelling of flash flood at wadi Samail, Oman. *Annu. Disaster Prev. Res. Inst. Kyoto Univ.* **2016**, *59*, 533–541.

88. Al Ruheili, A.; Dahm, R.; Radke, J. Wadi flood impact assessment of the 2002 cyclonic storm in Dhofar, Oman under present and future sea level conditions. *J. Arid Environ.* **2019**, *165*, 73–80. https://doi.org/10.1016/J.JARIDENV.2019.04.002.

89. Youssef, A.M.; Abu-Abdullah, M.M.; Alfadail, E.A.; Skilodimou, H.D.; Bathrellos, G.D. The devastating flood in the arid region a consequence of rainfall and dam failure: Case study, Al-Lith flood on 23th November 2018, Kingdom of Saudi Arabia. *Z. Für Geomorphol.* **2021**, *63*, 115–136. https://doi.org/10.1127/zfg/2021/0672.